博士論文

Common findings on postmortem computed tomography in atraumatic death; compared with antemortem computed tomography and pathological findings

（非外傷性患者における死後CTの正常所見についての検討

～生前CTと病理所見との対比～）

大熊　ひでみ

Contents

1. Abbreviations

3D	three-dimensional
AMCT	antemortem computed tomography
AUC	areas under the ROC curve
CI	confidence intervals
CPR	cardiopulmonary resuscitation
CT	computed tomography
CTR	cardiothoracic ratio
CTRa	cardiothoracic ratio measured on an axial image
CTRs	cardiothoracic ratio measured on the scout view
CXR	chest radiography
eGFR	estimated glomerular filtration rate
HU	Hounsfield units
MPR	multiplanar reconstruction
MRI	magnetic resonance imaging
PMCT	postmortem computed tomography
ROC	Receiver-operating characteristic
ROI	region of interest
SD	standard deviation
SVC	superior vena cava

2. List of publications

Permissions are granted for me to use all the articles for my doctoral thesis and to e-publish them at the UT repository.

1. “Heart wall is thicker on postmortem computed tomography than on antemortem computed tomography: the first longitudinal study”

Okuma H, Gonoi W, Ishida M, Shintani Y, Takazawa Y, Fukayama M, Ohtomo K.

PLoS One. 2013 Sep 27;8(9):e76026. → Chapter 6

2. “Comparison of attenuation of striated muscle between postmortem and antemortem computed tomography: results of a longitudinal study”

Okuma H, Gonoi W, Ishida M, Shirota G, Shintani Y, Abe H, Fukayama M, Ohtomo K.

PLoS One. 2014 Nov 3;9(11):e111457. → Chapter 7

3. “Greater thickness of the aortic wall on postmortem computed tomography compared with antemortem computed tomography: the first longitudinal study”

Okuma H, Gonoi W, Ishida M, Shintani Y, Takazawa Y, Fukayama M, Ohtomo K.

Int J Legal Med. 2014 Nov;128(6):987-93. → Chapter 8

4. “Comparison of the cardiothoracic ratio between postmortem and antemortem computed tomography”

Okuma H, Gonoi W, Ishida M, Shirota G, Kanno S, Shintani Y, Abe H, Fukayama M, Ohtomo K.

Leg Med (Tokyo). 2016; 10.1016/j.legalmed.2016.12.006 → Chapter 9

3. Abstract

As postmortem imaging has gained prominence as a supplement to traditional autopsy, it is important to understand the normal postmortem changes to enable the accurate evaluation of postmortem imaging. However, our knowledge of postmortem imaging findings is incomplete and no standards for interpreting the cardiovascular system were available prior to the present study. We conducted four consecutive studies, which investigated heart wall thickness, attenuation of the cardiac muscle, cardiothoracic ratio, and thickness of the aortic wall on postmortem computed tomography (CT) compared with antemortem CT. The Institutional Review Board approved these studies and informed consent was obtained from the next of kin. We studied subjects who underwent antemortem CT, postmortem CT, and autopsy between April 2009 and December 2011. Postmortem CT was performed < 23 h after death and was followed by pathological studies. We found a general greater thickness of the heart wall, greater attenuation of cardiac muscle, greater cardiothoracic ratio, and greater thickness of the aortic wall on postmortem CT compared with antemortem CT obtained in the same patients. These results caution us against overestimating cardiomegaly and mislabeling as pathological the normal postmortem changes of the cardiovascular system.

4. Introduction

It is important to determine the cause of death for many reasons. From a personal perspective, the next of kin wants to know why their family member died. From the perspective of the general population, knowing the cause of death may aid medical development, improve public health, and help detect otherwise overlooked crime-related deaths. Although traditional autopsy is the best approach to determine the cause of death, its use is declining worldwide [1]. In Japan, the autopsy rate was reported to be < 2% for hospital deaths, while the judicial autopsy rate was about 5% and the administrative autopsy rate was about 6.6%. Because the overall autopsy rate is quite low in Japan, the cause of death is not fully confirmed in many cases.

High-resolution imaging modalities such as computed tomography (CT) and magnetic resonance imaging (MRI) are increasingly being used as adjuncts to traditional forensic methods in postmortem studies [2-6]. In Japan, Shiotani et al introduced postmortem CT imaging in 1985 and presented their results of postmortem imaging about 15 years later [7-10]. In 2000, the Swiss forensic pathologist Thali introduced the term “virtopsy”, or virtual autopsy. In 2003, Ezawa et al reported the world’s first postmortem imaging study, which was conducted in Japan. The Japan Society of Autopsy Imaging was established in the same year. “Autopsy imaging” is now commonly used to describe postmortem imaging in Japan. In 2006, the world’s first autopsy imaging center was established in Chiba University. At least

17 other universities in Japan have since introduced autopsy imaging centers, including Sapporo Medical University, Tohoku University, Fukushima Medical University, Gunma University, Kanagawa Dental University, University of Fukui, Mie University, Kindai University, Kyoto Prefectural University of Medicine, Osaka University, Kobe University, Ehime University, Shimane University, Nagasaki University, Miyazaki University, Oita University, and Saga University. In addition, many Japanese community hospitals regularly perform postmortem imaging.

Postmortem imaging is now widely performed throughout Japan. One reason is that there are many CT and MRI machines in Japan and postmortem departments have very good access to these systems. Another reason is that postmortem imaging modalities can provide detailed images of organs and tissues within the body that cannot be obtained by superficial examination. These images may help the pathologist to determine whether or not to proceed with autopsy and improve the accuracy of the suspected cause of death.

The increasing frequency of child abuse and sophisticated crimes make it especially important to unravel the deceased's underlying disease, if any, and the actual cause of death. In 2012, new laws concerning cause of death investigation were established in Japan. These laws explicitly mentioned postmortem imaging. These laws recommend performing autopsy regardless of incidental factors, even without agreement from the next of kin. The laws also strongly recommend postmortem imaging in cases where autopsy is not possible for any

reason, highlighting the importance of postmortem imaging and giving valuable support for imaging.

The decreasing autopsy rate means postmortem imaging should be performed more frequently. However, clinical radiologists may find it difficult to interpret postmortem images because of specific and nonspecific postmortem signs on CT [11]. Now that diagnostic guidelines based on postmortem imaging are being established worldwide, it is important to understand the normal changes that occur on postmortem CT [12]. The postmortem CT features of several organs, including the cardiovascular system [13-16], brain [17], thyroid [18], adrenal gland [19], spleen [20], muscle [21], airway [22], and lung [23], have already been described. The normal postmortem features of the cardiovascular system have attracted particular interest because postmortem findings allow us to determine the causes of cardiovascular disease- or heart failure-related deaths, the most common causes of death.

Most postmortem imaging studies involved patients admitted for emergent reasons and/or external injury, where the researchers had limited information on the patients or it was impossible to compare the postmortem images with antemortem images. By contrast, most patients die in hospitals due to endogenic diseases after a long period of treatment. In such cases, the pathologist is provided with sufficient clinical information and often antemortem images. It is rare to have antemortem and postmortem images in patients who also undergo pathological autopsy, and we are fortunate to be able to compare this information in the same

patients. We believe that the results of my studies will help efforts to establish standards for assessing normal postmortem changes. I have conducted four consecutive studies examining the postmortem changes of the following cardiovascular features: thickness of the heart wall, attenuation of cardiac muscle, the cardiothoracic ratio, and the thickness of the aortic wall.

5. Materials and methods in common

The Institutional Review Board of the University of Tokyo Hospital approved this study (#2076). Written informed consent was obtained from the next of kin to use the clinical, pathological, and radiographic data in this study.

Antemortem CT imaging

In chapter 6, 7, and 8, all antemortem CT studies were performed on 64-detector-row helical CT scanners (Aquilion 64, Toshiba Medical Systems Corporation, Ohtawara, Japan; Discovery CT750 HD and LightSpeed VCT, GE Healthcare, Buckinghamshire, UK). In chapter 9, all antemortem CT scans were obtained using either of the three 64-slice helical CT scanners (Aquilion 64, Toshiba Medical Systems Corporation, Ohtawara, Japan; Discovery CT750 HD and LightSpeed VCT, GE Healthcare, Buckinghamshire, UK) or a 320-detector-row helical CT scanner (Aquilion ONE, Toshiba Medical Systems Corporation, Ohtawara, Japan). All CT scans were performed in the craniocaudal direction with the patient in the supine position with arms raised. The scan parameters were as follows: slice thickness, 5 mm; slice interval, 5 mm; rotation time, 0.5 s; and tube voltage, 120 kVp. Tube current was controlled automatically using Volume EC and Auto mA. Image reconstruction was performed at 0.5-mm intervals with a 350-mm field of view and a 512 × 512 image matrix.

Postmortem CT imaging

Whole-body postmortem CT studies were obtained in the craniocaudal direction without contrast medium using a four-detector-row CT scanner (Robusto, Hitachi Medical Corporation, Tokyo, Japan) in the helical mode. For all scans, the cadaver was laid in the supine position with arms placed on either side of the body. The scan parameters were as follows: slice thickness, 2.5 mm; slice interval, 1.25 mm; rotation time, 0.5 s; tube voltage, 120 kVp; and tube current, 250 mA. Images were reconstructed at 1.25 mm intervals with a 350 mm field of view and a 512 × 512 image matrix.

Interval between antemortem and postmortem imaging

We used the most recent available antemortem CT in each patient, which was mostly performed within a few months before death, although the maximum interval was 3.8 years for chapter 6 and 8.

Postmortem CT was performed within 23 hours after death, and was immediately followed by pathological studies.

6. “Greater thickness of the heart wall on postmortem computed tomography than on antemortem computed tomography”

Background

To my knowledge, the features of cardiac hypertrophy on postmortem CT have not been reported. My aim was to investigate wall thickening of the heart on postmortem CT in comparison with the antemortem CT findings, and in comparison with the pathological findings, in cases of non-traumatic in-hospital death.

Materials and Methods

Study design and subjects

A total of 97 patients who died non-traumatically in my academic tertiary-care hospital and who underwent antemortem CT, postmortem CT, and pathological autopsy between April 2009 and December 2010 were retrospectively enrolled in this study. Exclusion criteria were as follows: (a) age < 20 years; (b) cardiopulmonary resuscitation (CPR) performed; and (c) congenital heart disease, chronic heart failure, cardiomyopathy, cardiac hypertrophy, heart amyloidosis, or previous cardiovascular surgery. The final study population consisted of 57 adult human cadavers (40 male, 17 female); mean age at death was 66 years (range, 21–92 years; median, 71 years). All cadavers were placed in the supine position at room temperature

from the time of death until postmortem CT examination. Postmortem CT was performed at 81–1187 min (median 328 min) after death. In addition to these 57 cases, my colleagues and I also performed antemortem CT, postmortem CT, and pathological autopsy on 3 cadavers with dilated cardiomyopathy (2 male, 1 female; 22, 53, and 57 years at death).

Image interpretation

CT images were reviewed on a three-dimensional (3D) workstation (ZioTerm2009; Ziosoft, Inc., Tokyo, Japan) to obtain multiplanar reconstruction (MPR) images vertical to the long axis of the left ventricle, transecting the apex and the center of the mitral valve. A slice at approximately one third of the distance from the apex, corresponding to the pathological section of the heart, was chosen for analysis. Using the MPR images, my colleagues and I measured the cardiac chambers at five sites: anterior wall of the left ventricle, left ventricular free wall, posterior wall of the left ventricle, ventricular septum, and right ventricular wall (Fig. 1a-b). Image analysis was performed by two board-certified radiologists who were not provided with clinical information. The best fit was determined by agreement between the radiologists. The postmortem and most recent antemortem chest CT images were compared. The appropriateness of the measurements will be discussed in chapter 10.

Pathological analysis

Hearts were studied before formalin fixation on photographs printed with standard scale. Each heart was cross-sectioned into slices approximately 1 cm thick, and a slice at proximately one third of the distance from the apex was chosen for measurement. A surgical pathologist measured myocardial thickness of the anterior wall of the left ventricle, left ventricular free wall, posterior wall of the left ventricle, ventricular septum, and right ventricular wall according to conventional methods [24] at the minimum diameter of each site, excluding papillary muscles and epicardial fat (Fig. 1c). Additional measurements including the papillary muscles and epicardial fat were made at each site for further analysis. The postmortem CT and pathological slices were compared. Slices were determined to be positive for the presence of arteriosclerosis when coronary artery stenosis or atherosclerosis was found pathologically (positive, n = 34; negative, n = 23). The most strongly related cause of death (such as heart failure, respiratory failure, liver failure, loss of blood, or other) was decided based on the clinical course just before death and the pathological findings (heart failure, n = 7; respiratory failure, n = 32; liver failure, n = 4; blood loss, n = 2; other, n = 12). The heart was defined as the organ most related to the cause of death in the case of heart failure; cause of death was classified as ‘other’ in the case of respiratory failure, liver failure, loss of blood, or other causes.

Statistical analyses

The average values of the two raters were used for analysis. First I compared the measured values on antemortem CT with and without contrast medium by paired t-test, to assess whether I could combine the contrasted and non-contrasted antemortem CT data in further analysis. I then investigated differences between the measured values on antemortem CT and postmortem CT, as well as between those on postmortem CT and pathological measurements, by paired t-test. Postmortem change in heart wall thickness was defined in two ways: as the difference in heart wall thickness between postmortem CT and antemortem CT, and as the ratio of heart wall thickness on postmortem CT to that on antemortem CT. I analyzed postmortem change in heart wall thickness by unpaired t-test with the following three postmortem changes as confounding factors: gender, presence or absence of arteriosclerosis, and whether or not the heart was the organ most strongly related to the cause of death. Postmortem change in heart wall thickness was also analyzed by linear least squares regression with age and elapsed time since death as additional confounding factors. The level of statistical significance was set at 0.05. Family-wise error was corrected by Bonferroni's correction for each section. All statistical computing was performed using the free software R, version 3.0 (The R Foundation for Statistical Computing, Vienna, Austria, http://www.r-project.org/).

Fig. 1. Antemortem and postmortem measurements of the heart of a 60-year-old man.

(a). Multiplanar reconstruction image of antemortem CT.
(b). Multiplanar reconstruction image of postmortem CT.
(c). Photograph of the pathological cross-sectional slice.

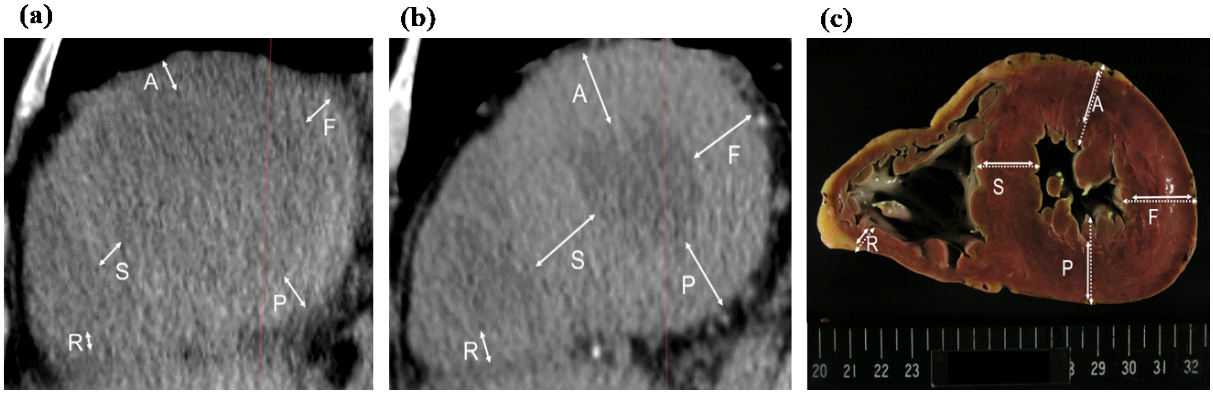

All three of these images represent the same plane.
Solid lines represent measurements without including papillary muscles or epicardial fat, according to conventional methods. Dotted lines represent measurements with papillary muscles and epicardial fat.
A, anterior wall of the left ventricle; F, left ventricular free wall; P, posterior wall of the left ventricle; S, ventricular septum; R, right ventricular wall

Results

The measured values for heart wall thickness on antemortem CT with and without contrast medium are summarized in Table 1. No significant differences were observed between antemortem CT with and without contrast medium at any site: anterior wall of the left ventricle, left ventricular free wall, posterior wall of the left ventricle, ventricular septum, or right ventricular wall. I thus combined the contrasted and non-contrasted antemortem CT data for further analysis: non-contrasted antemortem CT was used when it was available; otherwise, contrasted antemortem CT was used.

The measured values for heart wall thickness on antemortem CT and postmortem CT are summarized in Table 2. The heart wall was significantly thicker on postmortem CT than on antemortem CT, at all sites.

Pathologically measured values for heart wall thickness are summarized in Table 3. The heart wall was significantly thicker on postmortem CT than on pathology specimens when measured without papillary muscles or epicardial fat according to conventional methods. However, no significant differences were observed between measurements on postmortem CT and pathology specimens at any site when measurements included papillary muscles and epicardial fat.

Tables 4-6 summarize the association of postmortem change in heart wall thickness with each of gender, presence of arteriosclerosis, and the organ related to the cause of death.

Gender, presence of arteriosclerosis, and heart failure as the cause of death showed no statistically significant association with postmortem change in heart wall thickness.

Tables 7-8 show the results of correlation analysis for postmortem change in heart wall thickness with each of age and elapsed time since death, revealing no statistically significant correlation.

Tables 9-10 summarize postmortem change in heart wall thickness in the cases of dilated cardiomyopathy and in the controls. There was less postmortem change in heart wall thickness in cases of dilated cardiomyopathy compared with control cases.

Table 1. Heart wall thickness on antemortem CT with and without contrast medium

	Contrasted	Non-contrasted	p value
Anterior wall of the left ventricle (mm; mean ± SD)	10.0 ± 2.9	11.0 ± 1.6	0.25
Left ventricular free wall (mm; mean ± SD)	12.6 ± 3.1	11.0 ± 1.6	0.06
Posterior wall of the left ventricle (mm; mean ± SD)	13.3 ± 3.6	10.9 ± 1.8	0.04[#]
Ventricular septum (mm; mean ± SD)	11.1 ± 3.0	11.2 ± 1.7	0.86
Right ventricular wall (mm; mean ± SD)	4.0 ± 1.4	4.8 ± 0.9	0.13

Statistical analyses were performed by paired t-test.

SD, standard deviation; AMCT, antemortem computed tomography

[#]Statistically insignificant when family-wise error was corrected by Bonferroni's correction

Table 2. Heart wall thickness on antemortem CT and postmortem CT

	AMCT	PMCT	p value
Anterior wall of the left ventricle (mm; mean ± SD)	10.8 ± 2.8	17.1 ± 3.3	< 0.0001*
Left ventricular free wall (mm; mean ± SD)	12.1 ± 2.9	19.3 ± 3.5	< 0.0001*
Posterior wall of the left ventricle (mm; mean ± SD)	11.7 ± 2.8	18.2 ± 3.2	< 0.0001*
Ventricular septum (mm; mean ± SD)	11.5 ± 2.8	17.3 ± 3.6	< 0.0001*
Right ventricular wall (mm; mean ± SD)	4.7 ± 2.0	7.5 ± 2.6	< 0.0001*

Statistical analyses were performed by paired t-test.
SD, standard deviation; AMCT, antemortem computed tomography; PMCT, postmortem computed tomography
*Statistically significant

Table 3. Heart wall thickness on pathology specimens measured with and without papillary muscles and epicardial fat

	PMCT	Pathology(–)	p value[1]	Pathology(+)	p value[2]
Anterior wall of the left ventricle (mm; mean ± SD)	17.1 ± 3.3	12.8 ± 3.0	< 0.0001*	19.2 ± 5.2	0.02[#]
Left ventricular free wall (mm; mean ± SD)	19.3 ± 3.5	13.9 ± 3.0	< 0.0001*	20.5 ± 3.8	0.06
Posterior wall of the left ventricle (mm; mean ± SD)	18.2 ± 3.2	12.5 ± 2.8	< 0.0001*	19.3 ± 3.4	0.10
Ventricular septum (mm; mean ± SD)	17.3 ± 3.6	12.7 ± 3.0	< 0.0001*	17.8 ± 3.8	0.38
Right ventricular wall (mm; mean ± SD)	7.5 ± 2.6	4.1 ± 1.1	< 0.0001*	7.3 ± 1.1	0.61

Statistical analyses were performed by paired t-test.
p value[1], between PMCT and pathological specimen, without papillary muscles or epicardial fat
p value[2], between PMCT and pathological specimen, with papillary muscles and epicardial fat
SD, standard deviation; PMCT, postmortem computed tomography; pathology(–), without papillary muscles and epicardial fat; pathology(+), with papillary muscles and epicardial fat
*Statistically significant
[#]Statistically insignificant when family-wise error was corrected by Bonferroni's correction

Table 4. Association between postmortem change in heart wall thickness and gender

	M(PM–AM)	Fe(PM–AM)	p value	M(PM/AM)	Fe(PM/AM)	p value
A (mm; mean ± SD)	6.9 ± 3.8	5.0 ± 4.5	0.12	1.7 ± 0.5	1.6 ± 0.6	0.59
F (mm; mean ± SD)	7.2 ± 4.5	7.2 ± 4.0	0.98	1.6 ± 0.4	1.7 ± 0.4	0.54
P (mm; mean ± SD)	6.9 ± 3.5	5.7 ± 4.0	0.27	1.6 ± 0.4	1.6 ± 0.5	0.75
S (mm; mean ± SD)	6.4 ± 3.9	4.2 ± 3.7	0.05	1.6 ± 0.5	1.4 ± 0.4	0.11
R (mm; mean ± SD)	3.0 ± 2.3	2.2 ± 1.8	0.19	1.8 ± 0.7	1.6 ± 0.5	0.25

Statistical analyses were performed by unpaired t-test.
M, male; Fe, female; PM–AM, difference in heart wall thickness between postmortem computed tomography and antemortem computed tomography; PM/AM, ratio of heart wall thickness on postmortem computed tomography to that on antemortem computed tomography; SD, standard deviation; A, anterior wall of the left ventricle; F, left ventricular free wall; P, posterior wall of the left ventricle; S, ventricular septum; R, right ventricular wall

Table 5. Association between postmortem change in heart wall thickness and presence of arteriosclerosis

	(+)(PM–AM)	(–)(PM–AM)	p value	(+)(PM/AM)	(–)(PM/AM)	p value
A (mm; mean ± SD)	6.4 ± 4.6	6.2 ± 3.3	0.87	1.7 ± 0.6	1.7 ± 0.4	0.75
F (mm; mean ± SD)	7.2 ± 4.8	7.2 ± 3.4	0.98	1.7 ± 0.5	1.7 ± 0.4	0.86
P (mm; mean ± SD)	6.5 ± 4.2	6.6 ± 2.8	0.92	1.6 ± 0.4	1.7 ± 0.4	0.64
S (mm; mean ± SD)	5.8 ± 4.2	5.8 ± 3.8	0.96	1.5 ± 0.4	1.6 ± 0.5	0.59
R (mm; mean ± SD)	2.5 ± 2.1	3.3 ± 2.2	0.19	1.6 ± 0.5	1.9 ± 0.8	0.12

Statistical analyses were performed by unpaired t-test.
(+), with arteriosclerosis; (–), without arteriosclerosis; PM–AM, difference in heart wall thickness between postmortem computed tomography and antemortem computed tomography; PM/AM, ratio of heart wall thickness on postmortem computed tomography to that on antemortem computed tomography; SD, standard deviation; A, anterior wall of the left ventricle; F, left ventricular free wall; P, posterior wall of the left ventricle; S, ventricular septum; R, right ventricular wall

Table 6. Association between postmortem change in heart wall thickness and cause of death

	H(PM–AM)	O(PM–AM)	p value	H(PM/AM)	O(PM/AM)	p value
A (mm; mean ± SD)	5.9 ± 5.9	6.5 ± 3.8	0.38	1.5 ± 0.5	1.8 ± 0.5	0.28
F (mm; mean ± SD)	5.8 ± 6.7	7.4 ± 3.9	0.35	1.6 ± 0.6	1.7 ± 0.4	0.45
P (mm; mean ± SD)	5.6 ± 6.3	6.7 ± 3.3	0.50	1.5 ± 0.5	1.6 ± 0.4	0.29
S (mm; mean ± SD)	1.6 ± 0.5	5.8 ± 3.9	0.93	1.5 ± 0.4	1.6 ± 0.5	0.62
R (mm; mean ± SD)	1.9 ± 2.0	3.0 ± 2.2	0.24	1.4 ± 0.5	1.8 ± 0.6	0.16

Statistical analyses were performed by unpaired t-test.
H, died of heart failure; O, died of other than heart failure; PM–AM, difference in heart wall thickness between postmortem computed tomography and antemortem computed tomography; PM/AM, ratio of heart wall thickness on postmortem computed tomography to that on antemortem computed tomography; SD, standard deviation; A, anterior wall of the left ventricle; F, left ventricular free wall; P, posterior wall of the left ventricle; S, ventricular septum; R, right ventricular wall

Table 7. Correlation of association between postmortem change in heart wall thickness with age

	PM–AM	PM/AM
Anterior wall of the left ventricle	0.064	0.090
Left ventricular free wall	0.061	0.063
Posterior wall of the left ventricle	0.060	0.072
Ventricular septum	0.20	0.22
Right ventricular wall	0.086	0.060

Statistical analyses were performed by linear least squares regression.
PM–AM, difference in heart wall thickness between postmortem computed tomography and antemortem computed tomography; PM/AM, ratio of heart wall thickness on postmortem computed tomography to that on antemortem computed tomography

Table 8. Correlation of association between postmortem change in heart wall thickness with elapsed time since death

	PM–AM	PM/AM
Anterior wall of the left ventricle	0.21	0.18
Left ventricular free wall	0.11	0.11
Posterior wall of the left ventricle	0.10	0.067
Ventricular septum	0.16	0.10
Right ventricular wall	0.15	0.04

Statistical analyses were performed by linear least squares regression.
PM–AM, difference in heart wall thickness between postmortem computed tomography and antemortem computed tomography; PM/AM, ratio of heart wall thickness on postmortem computed tomography to that on antemortem computed tomography

Table 9. Heart wall thickness on antemortem CT and postmortem CT in dilated cardiomyopathy

	AMCT	PMCT
Anterior wall of the left ventricle (mm; mean ± SD)	14.3 ± 1.9	15.7 ± 2.9
Left ventricular free wall (mm; mean ± SD)	12.8 ± 1.4	14.3 ± 1.3
Posterior wall of the left ventricle (mm; mean ± SD)	13.4 ± 2.4	14.8 ± 2.4
Ventricular septum (mm; mean ± SD)	12.6 ± 3.3	16.4 ± 1.5
Right ventricular wall (mm; mean ± SD)	5.4 ± 0.6	7.5 ± 1.8

SD, standard deviation; AMCT, antemortem computed tomography; PMCT, postmortem computed tomography

Table 10. Postmortem change in heart wall thickness in cases of dilated cardiomyopathy and in controls

	DC(PM–AM)	C(PM–AM)	DC(PM/AM)	C(PM/AM)
Anterior wall of the left ventricle (mm; mean ± SD)	1.4 ± 4.6	6.5 ± 0.8	1.1 ± 0.3	1.6 ± 1.3
Left ventricular free wall (mm; mean ± SD)	1.5 ± 2.7	7.3 ± 0.6	1.1 ± 0.2	1.6 ± 1.1
Posterior wall of the left ventricle (mm; mean ± SD)	2.8 ± 3.4	6.6 ± 0.0	1.2 ± 0.3	1.6 ± 1.0
Ventricular septum (mm; mean ± SD)	3.8 ± 4.0	6.1 ± 1.2	1.4 ± 0.4	1.5 ± 1.4
Right ventricular wall (mm; mean ± SD)	2.1 ± 1.4	2.8 ± 0.5	1.4 ± 0.2	1.6 ± 1.2

SD, standard deviation; PM–AM, difference in heart wall thickness between postmortem computed tomography and antemortem computed tomography; PM/AM, ratio of heart wall thickness on postmortem computed tomography to that on antemortem computed tomography; DC, dilated cardiomyopathy; C, control

Discussion

Because of the obvious differences in appearance between contrast-enhanced and plain images, I evaluated whether the measured values of heart wall thickness were equivalent between these two sets of images. No significant difference was found, which enabled me to use either contrasted or non-contrasted images to obtain measurements.

While several previous studies have evaluated the postmortem changes of the cardiovascular system [25-28], few studies have focused on heart wall thickness. Hutchins et al. [29] measured ventricular wall thickness on stereoscopic radiographs of hearts obtained at autopsy, and concluded that the left ventricular free wall is the thickest, followed by the interventricular septum; the right ventricular free wall is the thinnest. The present results are generally in agreement with theirs.

In the present study, the heart wall was significantly thicker on postmortem CT than on antemortem CT in the same patients. Lewy et al. [30] reported that postmortem CT showed no specific findings for rigor mortis, and that rigor did not affect the CT attenuation, size, or shape of skeletal muscles. However, it is well known in forensic medicine and pathology that rigor mortis causes contraction of the heart, which manifests as a hypertrophic appearance of the ventricular walls [31-33]. Postmortem change in heart wall thickness should be associated with elapsed time since death if rigor mortis principally accounts for heart wall thickness on postmortem CT, because the presence and degree of rigor mortis generally changes in the

period between 1–2 hours and 24–36 hours after death [34]. All postmortem CT scanning in the present study was performed between 1 and 20 hours post mortem, which coincides with the timing of rigor mortis. My results showed that the heart wall becomes thicker post mortem, which is consistent with the knowledge in forensic medicine and pathology that the ventricular walls appear hypertrophic after death. However, because the present study revealed few associations between postmortem change in heart wall thickness and elapsed time after death, it is possible that this change may occur within the first few hours or even minutes after death, which is earlier than the observation time of the present study.

I also investigated possible confounding factors of postmortem change such as gender, presence of arteriosclerosis, the organ most strongly related to cause of death, and age. There was little association between these factors and postmortem change in heart wall thickness, which indicates that change in heart wall thickness is a general postmortem finding regardless of these factors.

Dilated cardiomyopathy is characterized by ventricular chamber enlargement and systolic dysfunction with normal left ventricular wall thickness [35]. The histologic features of dilated cardiomyopathy are nonspecific, and pathological findings range from minimal change in myocyte size to typical features of myofiber loss, interstitial fibrosis, and marked change in myofiber size [36]. It has been clarified that dilated cardiomyopathy is partly caused by mutations in the genes that encode for proteins of the myocyte contractile apparatus, the

myocyte cytoskeleton, and nuclear envelope, as well as proteins involved in calcium homeostasis [37]. Because the myocardium is injured and degenerates to various extents in dilated cardiomyopathy, we would expect to observe reduced postmortem change in heart wall thickness in these cases compared with controls, which is confirmed by the results of the present study. Furthermore, this leads to the supposition that ante mortem myocardial volume or thickness is positively correlated to postmortem change in heart wall thickness, although no correlation was found for confounding factors of postmortem change such as gender, presence of arteriosclerosis, the organ related to the cause of death, and age.

The heart wall was significantly thicker on postmortem CT than on pathology specimens when measured by conventional mensuration, which did not include papillary muscles or epicardial fat. However, no significant differences were observed between measurements on postmortem CT and pathology specimens when measurements included papillary muscles and epicardial fat. This could be because the resolution of the CT images was not high enough to enable distinction of papillary muscles and epicardial fat from myocardia, and because heart wall measurements on postmortem CT had included these elements.

Cardiac motion artifact is a major concern on antemortem CT that clearly does not arise on postmortem CT. Because I did not use electrocardiographic triggering on antemortem CT, these images were a composite of systolic and diastolic phases. According to the duration of each phase, it is assumed that on antemortem CT the systolic phase comprised approximately

0.4 of the entire cardiac cycle, while the other 0.6 was diastolic phase [38]. In contrast, the heart outlines on postmortem CT are considered to be close to those during the diastolic phase, because mean circulatory pressure of deceased subjects (approximately 7 mmHg) is similar to the end-diastolic pressure of the right or left ventricle of living subjects [27]. The heart wall becomes 40% to 60% thicker in the systolic phase compared with the diastolic phase [39], while in the present study, it was approximately 60% thicker on postmortem CT compared with antemortem CT. If there were no postmortem changes, then heart wall thickness should have been noticeably thinner on postmortem CT than on antemortem CT, which is the opposite to what was shown in the present results.

My study has another limitation. I did not consider underlying disease, preservation of cadavers, atmospheric temperature, or humidity, among other factors, which do affect postmortem changes [40, 41]. However, I consider that these factors would have had little effect on my conclusion, because I excluded heart disease from analysis and all the cadavers were preserved under automatically regulated conditions at our hospital.

Conclusions

This is the first longitudinal study to elucidate that the heart wall is significantly thicker on postmortem CT than on antemortem CT in cases of non-traumatic in-hospital death. Furthermore, the postmortem changes on CT were supported by the pathological findings.

7. “Comparison of attenuation of cardiac muscle between postmortem and antemortem computed tomography”

Background

To my knowledge, there are no reports describing the postmortem changes in CT attenuation of cardiac muscle. Therefore, I conducted a quantitative study in which I compared the attenuation of cardiac muscle between postmortem and antemortem CT in patients who died in hospital from nontraumatic causes.

Materials and Methods

Study design and subjects

A total of 73 patients who died from nontraumatic causes in my academic tertiary care hospital and who underwent unenhanced chest antemortem CT, postmortem CT, and pathological autopsy between April 2009 and December 2010 were retrospectively enrolled in this study. Potential donors were excluded for any of the following reasons: (a) age < 20 years; (b) treatment with cardiopulmonary resuscitation; (c) diagnosis of congenital heart disease, chronic heart failure, cardiomyopathy, cardiac hypertrophy, or heart amyloidosis; prior cardiovascular surgery; or diagnosis of muscular disorders, such as amyotrophic lateral sclerosis, muscular dystrophy, myositis, or myasthenia. Criterion (c) was confirmed by

pathological autopsy. After applying these exclusion criteria, 33 adult human cadavers (22 males, 11 females) were included in this study. The mean age at death was 66 years (range, 21–92 years; median, 72 years). All cadavers were placed in the supine position at room temperature from the time of death until postmortem CT. Antemortem CT was performed at a median of 17 days before death (range, 1–184 days). Postmortem CT was performed at a median of 464 min after death (range, 94–1175 min), followed by pathological autopsy.

Image interpretation

All images were interpreted by a radiologist who was not provided with clinical information. The postmortem and most recent antemortem unenhanced chest CT images were compared. CT images were reviewed on a three-dimensional workstation (ZioTerm2009, Ziosoft, Inc., Tokyo, Japan) to obtain multiplanar reconstruction images perpendicular to the line transecting the apex and the center of the mitral valve. A slice at approximately one third of the distance from the apex, corresponding to a pathological section of the heart, was chosen for the analysis. Using the multiplanar reconstruction images, my research group measured CT attenuation (in Hounsfield units; HU) at three points in each of the following four cardiac muscle sites: anterior wall of the left ventricle, left ventricular free wall, posterior wall of the left ventricle, and the ventricular septum (Fig. 2a-b). The mean values of the three points at each site were calculated. The CT attenuation (in HU) was also determined for the pectoralis

major muscle and the erector spinae muscle at the level of the aortic arch (Fig. 3a-b). CT attenuation was measured by setting a circular region of interest (ROI) to the center of each muscle. ROI size was as large as possible without being affected by partial volume phenomena, and the average CT attenuation within the ROI was used for analysis.

Statistical analyses

I compared the CT attenuation of six sites of striated muscle (i.e., four cardiac muscle sites: anterior wall of the left ventricle, left ventricular free wall, posterior wall of the left ventricle, ventricular septum; and two skeletal muscle sites: pectoralis major muscle and erector spinae muscle) between antemortem CT and postmortem CT using paired *t* tests. Significant differences among the four cardiac muscle sites were determined using Friedman's test. Significant differences between the two skeletal muscle sites were determined using the paired *t* tests. Significant differences between the group of cardiac muscles and that of skeletal muscles were analyzed by unpaired *t* tests. Postmortem change in the CT attenuation of striated muscle was defined as the ratio of CT attenuation of striated muscle on postmortem CT to that on antemortem CT. I used the unpaired t-test to analyze postmortem change in the CT attenuation of striated muscle with gender, and linear least squares regression for that with age and elapsed time since death. The level of statistical significance was set at 0.05. Family-wise error was corrected by Bonferroni's correction for each section. All statistical analyses

were performed using R version 3.0 (The R Foundation for Statistical Computing, Vienna, Austria; http://www.r-project.org/).

Fig. 2. Antemortem and postmortem CT images of the heart in a representative patient.

(a). Multiplanar reconstruction image obtained by antemortem CT.
(b). Multiplanar reconstruction image obtained by postmortem CT.

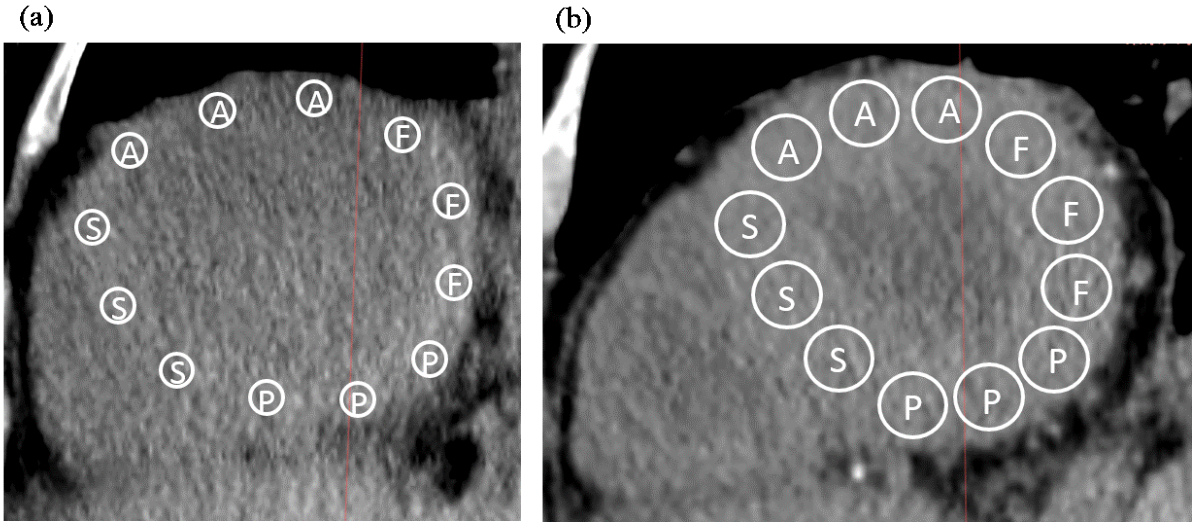

Both images were obtained in same plane.
A, anterior wall of the left ventricle; F, left ventricular free wall; P, posterior wall of the left ventricle; S, ventricular septum.

Fig. 3. Antemortem and postmortem CT images of the pectoralis major muscle and the erector spinae muscle in a representative patient.

(a). Antemortem CT.
(b). Postmortem CT.

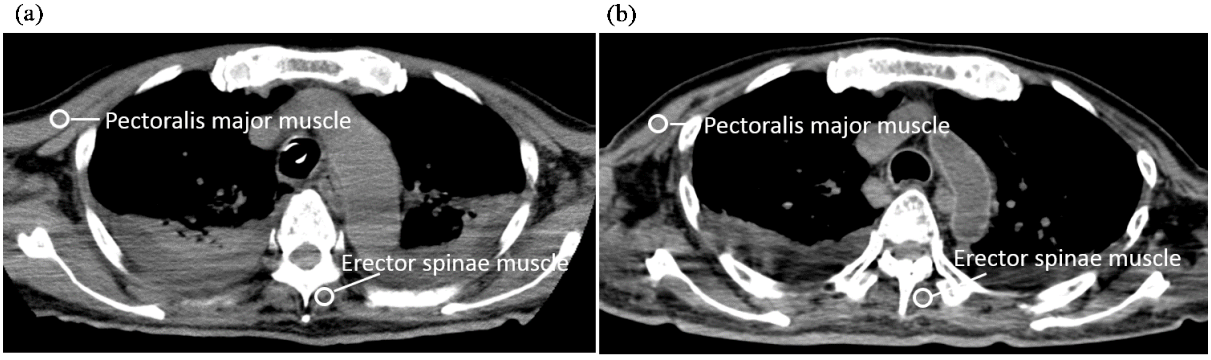

Both images were obtained at the level of the aortic arch.
PMM, pectoralis major muscle; ESM, erector spinae muscle.

Results

The CT attenuation values (in HU) of the four cardiac muscle sites and the two skeletal muscle sites on antemortem and postmortem CT are shown in a scatter plot (Fig. 4a-b). These results are also summarized in Table 11. Both cardiac and skeletal muscle showed significantly greater attenuation on postmortem CT than on antemortem CT. The Friedman test showed that there were no significant differences in CT attenuation among the four sites of cardiac muscle either on antemortem or on postmortem CT. There were also no significant differences in CT attenuation between the two sites of skeletal muscle either on antemortem or on postmortem CT. There were significant differences in CT attenuation between the cardiac and skeletal muscle groups on antemortem CT ($P < 0.001$) but not on postmortem CT.

Table 12 summarizes the association of postmortem change in the CT attenuation of striated muscle with gender. Gender showed no statistically significant association with postmortem change in the CT attenuation of striated muscle, at any of the tested sites.

Table 13 shows the results of correlation analysis for postmortem change in the CT attenuation of striated muscle with each of age and elapsed time since death. No statistically significant correlation was found at any site.

Fig. 4. Scatter plot of the CT attenuation values of cardiac and skeletal muscle on antemortem and postmortem CT.

(a). Cardiac muscle.
(b). Skeletal muscle.

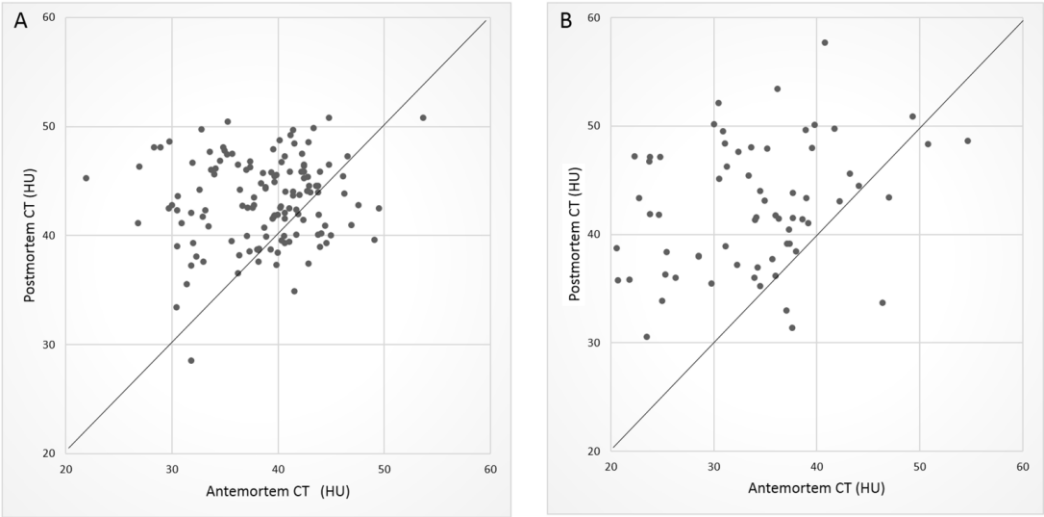

Table 11. Comparison of striated muscle attenuation in four cardiac muscle sites, the pectoralis major muscle, and the erector spinae muscle, between antemortem CT and postmortem CT.

Site	Antemortem CT attenuation (HU)	Postmortem CT attenuation (HU)	*P* value*
Cardiac muscle			
Anterior wall of the left ventricle	36.8 ± 6.2	42.5 ± 4.6	< 0.001
Left ventricular free wall	38.1 ± 6.2	44.1 ± 3.7	< 0.001
Posterior wall of the left ventricle	40.0 ± 3.8	43.8 ± 3.7	< 0.001
Ventricular septum	39.6 ± 3.4	42.5 ± 3.2	< 0.001
Skeletal muscle			
Pectoralis major muscle	33.7 ± 6.8	43.3 ± 5.9	< 0.001
Erector spinae muscle	34.1 ± 8.0	41.7 ± 5.6	< 0.001

Values are presented as the mean ± standard deviation.
*Paired *t* tests.
CT, computed tomography; HU, Hounsfield units

Table 12. Association between postmortem change in the CT attenuation of striated muscle and gender.

Site	Male (PM/AM)	Female (PM/AM)	P value
Cardiac muscle			
Anterior wall of the left ventricle	1.1 ± 0.2	1.3 ± 0.3	0.09
Left ventricular free wall	1.1 ± 0.2	1.3 ± 0.2	0.03#
Posterior wall of the left ventricle	1.1 ± 0.1	1.2 ± 0.2	0.04#
Ventricular septum	1.1 ± 0.1	1.1 ± 0.1	0.10
Skeletal muscle			
Pectoralis major muscle	1.3 ± 0.3	1.1 ± 0.3	0.08
Erector spinae muscle	1.4 ± 0.3	1.3 ± 0.3	0.29

Statistical analyses were performed by unpaired t-test.
Values are presented as the mean ± standard deviation.
CT, computed tomography; HU, Hounsfield units; PM/AM, ratio of CT attenuation of striated muscle on postmortem computed tomography to that on antemortem computed tomography
#Statistically insignificant when family-wise error was corrected by Bonferroni's correction

Table 13. Correlation of association between postmortem change in the CT attenuation of striated muscle with age and with elapsed time since death.

Site	Age	Elapsed time since death
Cardiac muscle		
Anterior wall of the left ventricle	0.79	0.12
Left ventricular free wall	0.98	0.34
Posterior wall of the left ventricle	0.30	0.05
Ventricular septum	0.38	0.32
Skeletal muscle		
Pectoralis major muscle	0.09	0.45
Erector spinae muscle	0.51	0.34

Statistical analyses were performed by linear least squares regression.
CT, computed tomography

Discussion

Although several studies have evaluated the postmortem changes of the cardiovascular system [15, 16, 25-28], few studies have examined the changes in CT attenuation. Shiotani et al. [26] reported that the attenuation of the aortic wall was greater on postmortem CT than on antemortem CT. They also reported that compression of aortic wall components, including collagen fibers, elastic fibers, and smooth muscle, may contribute to the hyperattenuation on postmortem CT. Okuma et al. [15] reported that the heart wall is thicker on postmortem CT than on antemortem CT, which suggests that postmortem contraction of cardiac muscle may cause increase the attenuation of cardiac muscle on postmortem images, as observed in my study.

In the present study, the CT attenuation of the pectoralis major muscle and the erector spinae muscle was significantly greater on postmortem CT than on antemortem CT in the same patients. Lewy et al. [30] reported that postmortem CT did not depict findings specific for rigor mortis, and that rigor did not affect CT attenuation, or the size and shape of skeletal muscles. However, it is well known in the fields of forensic medicine and pathology that rigor mortis causes contraction of striated muscle [33]. Because CT attenuation is affected by the density of muscle [42], the greater attenuation on postmortem CT than on antemortem CT is consistent with the contraction of striated muscle in rigor mortis.

There were no significant intra-group (among the four cardiac muscle sites or between the two skeletal muscle sites) differences in CT attenuation either on antemortem or postmortem CT. Even though they are named differently, the properties of cardiac muscle at different sites in the heart can be quite similar. Regarding the two sites of skeletal muscle, the pectoralis major and erector spinae muscles may also show similar CT attenuation values. Muscles are known to exhibit broad regional differences in muscle fiber density [43, 44] and in CT attenuation [45, 46]. I would have observed a wider variety of CT attenuation values in the group of skeletal muscle if more muscle regions had been added to the analysis.

Antemortem CT attenuation was significantly different between the cardiac and skeletal muscle groups. Because of the marked differences in cardiac and skeletal muscle in terms of their physiological properties as well as their pathological responses, the difference in CT attenuation between these two categories of muscle could reflect these differences in properties. The broad regional differences in muscle fiber density [43, 44] and CT attenuation [45, 46] mentioned earlier mean that the significant differences in antemortem CT attenuation among muscles in different regions detected in this study are to be expected. Although Bulcke et al. [45] and Termote et al. [46] reported similar findings—that the sternocleidomastoideus and iliopsoas are characterized by high attenuation and the gracilis and triceps surae are characterized by low attenuation—there were large differences in the measured CT values for

the same muscles. Therefore, we cannot compare the absolute values determined in this study with those of previous studies.

Somewhat unexpectedly, we found no significant differences in postmortem CT attenuation between the cardiac and skeletal muscle groups. One possible explanation is that rigor mortis resulted in marked contraction of the striated muscles, abolishing any possible differences between individual striated muscles on postmortem CT.

If rigor mortis is the principal cause of the hyperattenuation of striated muscle on postmortem CT, then postmortem change in the CT attenuation of striated muscle should be associated with elapsed time since death, because the presence and degree of rigor mortis generally changes in the period between 1–2 hours and between 24–36 hours after death [34]. In the present study, all postmortem CT scanning was performed between 1.5 and 20 hours post mortem, which coincides with the timing of rigor mortis. However, my results revealed few associations between postmortem change in the CT attenuation of striated muscle and elapsed time since death. One possibility for this finding is that the total number of patients analyzed in the study was too small to show a positive association.

I also investigated possible confounding factors of postmortem change such as gender and age. The associations between these factors and postmortem change in the CT attenuation of striated muscle were not statistically significant, which indicates that hyperattenuation of striated muscle is a general postmortem finding regardless of gender or age.

Interscanner variability of CT attenuation values (i.e., HU) is an issue that needs to be considered [47, 48], although almost all CT scanners show some intrascanner variability in CT attenuation values [49]. Recent technological innovations, however, may overcome these problems because some studies have shown negligible interscanner variability in terms of CT attenuation values [50]. Although CT attenuation values may not be directly compared between antemortem and postmortem CT because I used different scanners at each time, I fixed the tube voltage at 120 kVp, which should help to reduce the variability. Of course, the significant differences in CT attenuation values between antemortem and postmortem CT cannot be explained without considering postmortem changes if there is any interscanner or intrascanner variability.

My study has some other limitations. Motion artifacts from the heart may affect antemortem CT but do not affect postmortem CT. It is also possible that underlying diseases, cadaver preservation, atmospheric conditions (e.g. temperature or humidity), or other factors might contribute to the differences observed postmortem [40, 41]. However, some of these factors are unlikely to affect my conclusions because I excluded patients with cardiovascular or muscular diseases from the study, which was confirmed by the pathological autopsy, and all of the cadavers were preserved in accordance with the regulations used at our hospital.

Conclusions

This is the first longitudinal study to show that striated muscle exhibits significantly greater attenuation on postmortem CT than on antemortem CT in patients who died in hospital from nontraumatic causes.

8. “Greater thickness of the aortic wall on postmortem computed tomography compared with antemortem computed tomography”

Background

Though the postmortem CT findings of the aorta have been reported [25, 26, 28, 51], to my knowledge, postmortem changes of the aorta are not previously reported in terms of wall thickness comparing the postmortem and antemortem features. My aim was to quantitatively investigate wall thickening of the aorta by comparing postmortem CT and antemortem CT findings in the same patients who died non-traumatically.

Materials and Methods

Study design and subjects

A total of 97 patients who died non-traumatically in my academic tertiary-care hospital and underwent antemortem CT, postmortem CT, and pathological autopsy between April 2009 and December 2010 were retrospectively enrolled in this study. Exclusion criteria were as follows: (a) age <20 years; (b) cardiopulmonary resuscitation (CPR) performed; (c) cardiovascular disease such as aortic aneurysm, aortic dissection, or Marfan syndrome; or previous cardiovascular surgery. Criterion (c) was confirmed by pathological autopsy. The final study population consisted of 57 adult human cadavers (40 male, 17 female); mean age

at death was 66 years (range, 21–92 years; median, 71). 16 patients underwent plain antemortem CT, while 41 underwent contrast-enhanced antemortem CT; among those, 10 patients with moderate renal failure on the basis of estimated glomerular filtration rate (eGFR) as 31-60, 15 patients with severe renal failure (eGFR <30). All cadavers were placed in the supine position at room temperature from the time of death until postmortem CT examination. Plain antemortem CT was performed at 1-18 days (median, 7 day) before death. Contrast-enhanced antemortem CT was performed at 2-1395 days (median, 138 day) before death. Postmortem CT was performed at 81–1187 min (median, 328 min) after death, followed by pathological autopsy.

Image interpretation

Images (two-dimensional axial datasets) were interpreted at a DICOM viewer (zioTerm2009; Ziosoft, Inc., Tokyo, Japan). Image analysis was performed by a board-certified radiologist who was not provided with clinical information. The postmortem and most recent antemortem chest CT images were compared. I evaluated wall thickness (at the 3 and 9 o'clock positions) and the outer diameter (along major and minor axes) of the descending aorta at the level of the tracheal bifurcation on both antemortem CT and postmortem CT, in each patient (Fig. 5a–d). Wall thickness of superior vena cava (SVC) along major and minor axes was measured at the level of azygos arch on both antemortem CT

and postmortem CT, in each patient (Fig. 6a-b). Two cross-sectional measurements were obtained at the level of the tracheal bifurcation in each patient on both antemortem CT and postmortem CT, using the manual-trace method: the area within the inner wall and the area within the outer wall (Fig. 7a-b). Cross-sectional area of the aortic wall was defined as the difference between these two areas.

Statistical analyses

First I compared aortic wall thickness on antemortem CT with and without contrast medium by paired t-test, to assess whether I could combine the contrasted and non-contrasted antemortem CT data in further analysis. I then investigated differences between aortic wall thickness on antemortem CT and postmortem CT, as well as those between diameter of the aorta on antemortem CT and postmortem CT, by paired t-test. Postmortem change in aortic wall thickness and diameter of the aorta was defined in two ways: as the difference in aortic wall thickness and diameter of the aorta between postmortem CT and antemortem CT, and as the ratio of aortic wall thickness and diameter of the aorta on postmortem CT to that on antemortem CT. I analyzed the correlation between postmortem change in aortic wall thickness and diameter of the aorta by linear least squares regression. Differences between wall thickness of SVC on antemortem CT and postmortem CT were investigated by paired t-test. Further, I compared the area within the inner wall and the area within the outer wall on

antemortem CT and postmortem CT, as well as cross-sectional area of the aortic wall on antemortem CT and postmortem CT, by paired t-test. The level of statistical significance was set at 0.05. All statistical computing was performed using the free software R, version 3.0 (The R Foundation for Statistical Computing, Vienna, Austria, http://www.r-project.org/).

Fig. 5. Antemortem and postmortem CT images of a 75-year-old man.

(a). Antemortem CT at the level of the tracheal bifurcation.
(b). Enlarged view of (a).
(c). Postmortem CT at the level of the tracheal bifurcation.
(d). Enlarged view of (c).

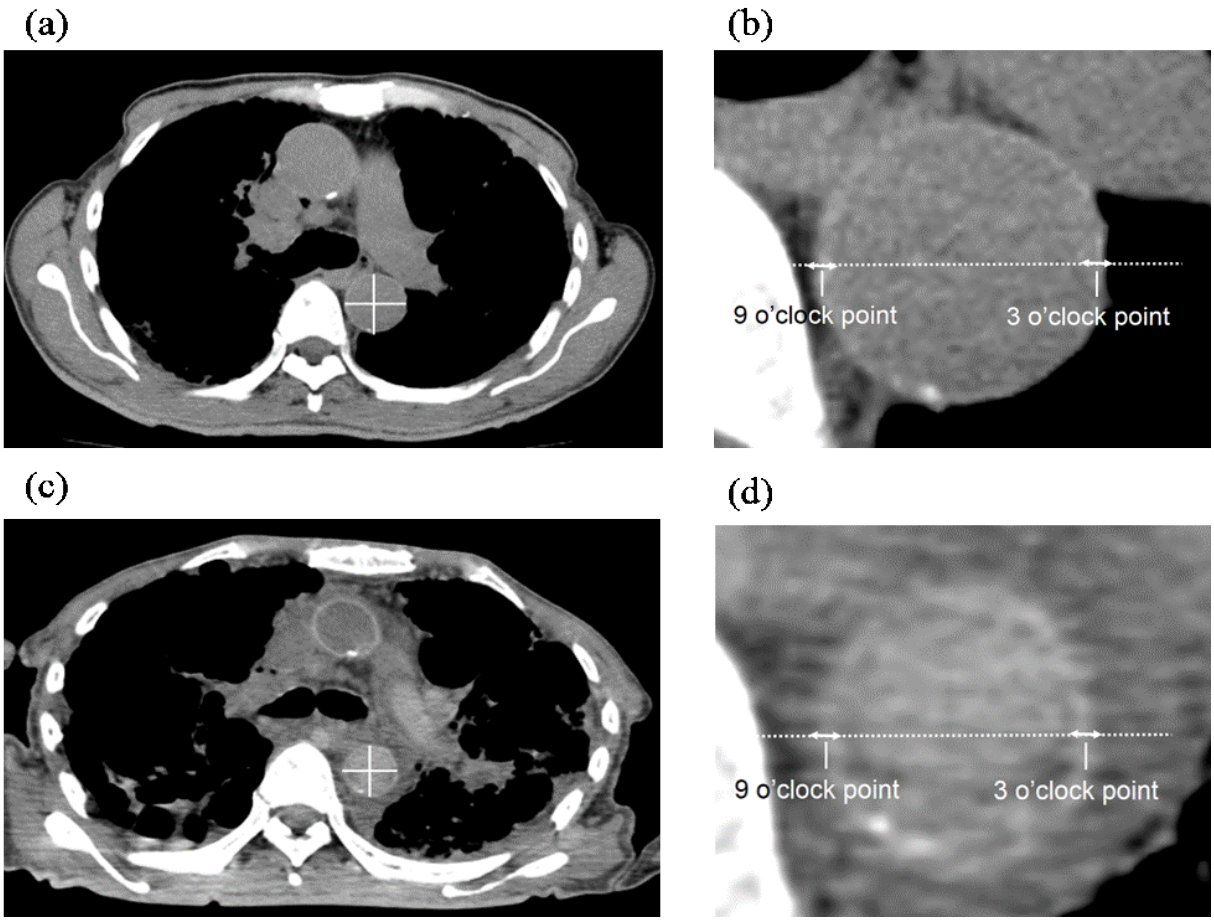

Solid lines represent measurements of outer diameter of the aorta along major and minor axes. Aortic wall thickness is measured at the 3 o'clock point and the 9 o'clock point.

Fig. 6. Antemortem and postmortem CT measurements of wall thickness of superior vena cava along major and minor axes.

(a). Antemortem CT at the level of azygos arch
(b). Postmortem CT at the level of azygos arch

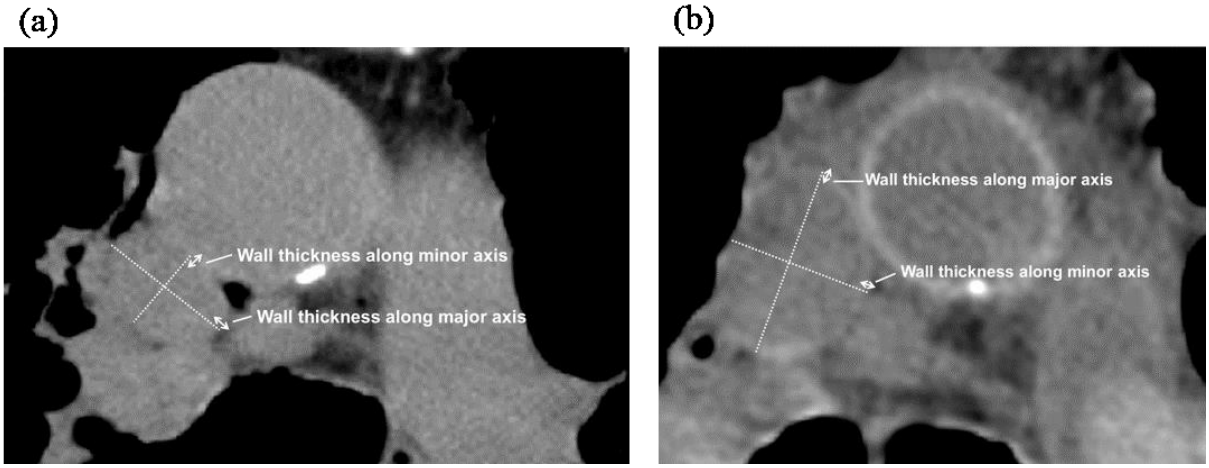

Fig. 7. CT image showing the two cross-sectional aortic measurements obtained on antemortem and postmortem CT: the area within the inner aortic wall (dotted line) and the area within the outer aortic wall (solid line).

(a). Antemortem CT at the level of the tracheal bifurcation.
(b). Postmortem CT at the level of the tracheal bifurcation.

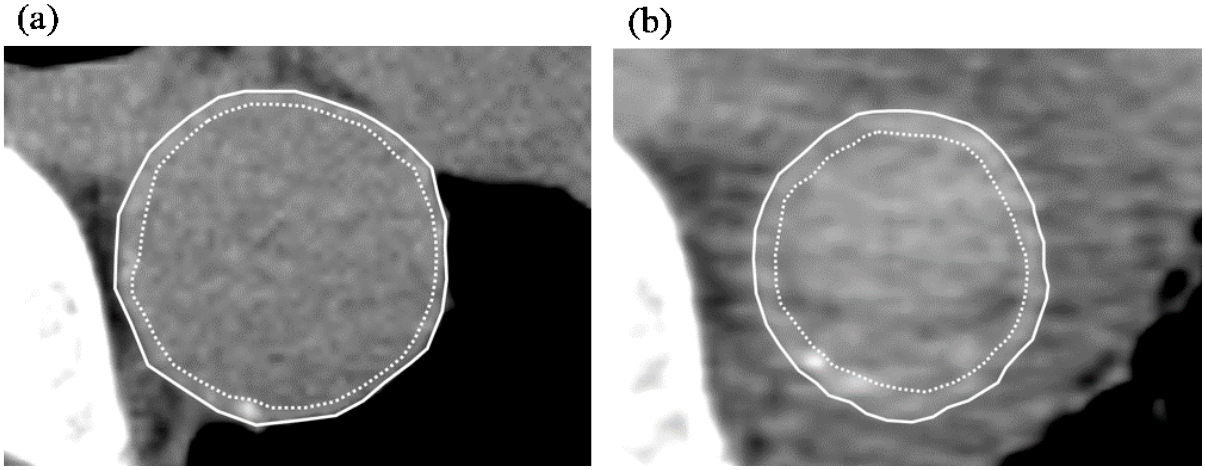

Results

The measured values for aortic wall thickness on antemortem CT with and without contrast medium are summarized in Table 14. No significant differences were observed between antemortem CT with and without contrast medium at either measurement point. I thus combined the contrasted and non-contrasted antemortem CT data for further analysis: non-contrasted antemortem CT was used when it was available; otherwise, contrasted antemortem CT was used.

The measured values for aortic wall thickness on antemortem CT and postmortem CT are summarized in Table 15. The aortic wall was significantly thicker on postmortem CT than on antemortem CT at both measurement points.

The measured values for the outer diameter of the aorta along major and minor axes are summarized in Table 16. The outer diameter of the aorta was significantly decreased on postmortem CT than on antemortem CT along both major and minor axes.

Table 17 shows the results of correlation analysis for postmortem change in aortic wall thickness and diameter of the aorta, revealing no statistically significant correlation.

The measured values for wall thickness of SVC along major and minor axes on antemortem CT and postmortem CT are summarized in Table 18. The wall of SVC was significantly thinner on postmortem CT than on antemortem CT at both measurement points.

Table 19 summarizes the results of measured area within the inner aortic wall and that within the outer aortic wall on antemortem CT and postmortem CT. Both values were significantly less on postmortem CT compared with antemortem CT. The ratio of cross-sectional area of the aortic wall on postmortem CT to that on antemortem CT was larger for the area within the outer wall compared with that for the area within the inner wall.

Table 20 summarizes measurements of cross-sectional area of the aortic wall on antemortem CT and postmortem CT. There was no statistically significant difference in cross-sectional area of the aortic wall between antemortem CT and postmortem CT.

Table 14. Aortic wall thickness on antemortem CT with and without contrast medium

	Contrast-enhanced	Plain	p value
3 o'clock point (mm; mean±SD)	1.7±0.7	1.7±0.6	0.97
9 o'clock point (mm; mean±SD)	1.8±0.6	2.0±0.5	0.19

Statistical analyses were performed by paired t-test.
SD, standard deviation; AMCT, antemortem computed tomography

Table 15. Aortic wall thickness on antemortem CT and postmortem CT

	AMCT	PMCT	p value
3 o'clock point (mm; mean±SD)	1.9±0.7	2.6±0.7	<0.0001*
9 o'clock point (mm; mean±SD)	1.8±0.6	2.6±0.7	<0.0001*

Statistical analyses were performed by paired t-test.
SD, standard deviation; AMCT, antemortem computed tomography; PMCT, postmortem computed tomography
*Statistically significant

Table 16. Outer diameter of the aorta along major and minor axes on antemortem CT and postmortem CT

	AMCT	PMCT	p value
major (mm; mean±SD)	28.4±4.3	23.7±3.5	<0.0001*
minor (mm; mean±SD)	26.8±4.0	20.9±4.2	<0.0001*

Statistical analyses were performed by paired t-test.
SD, standard deviation; AMCT, antemortem computed tomography; PMCT, postmortem computed tomography
*Statistically significant

Table 17. Correlation between aortic wall thickness and diameter of the aorta

PM-AM	PM/AM
0.13	0.092

Statistical analyses were performed by linear least squares regression.
PM–AM, correlation when postmortem change was defined as the difference between postmortem computed tomography and antemortem computed tomography; PM/AM, correlation when postmortem change was defined as the ratio on postmortem computed tomography to that on antemortem computed tomography

Table 18. Wall thickness of superior vena cava on antemortem CT and postmortem CT

	AMCT	PMCT	p value
major (mm; mean±SD)	1.2±0.3	1.0±0.3	<0.001*
minor (mm; mean±SD)	1.2±0.3	1.0±0.3	<0.001*

Statistical analyses were performed by paired t-test.
SD, standard deviation; AMCT, antemortem computed tomography; PMCT, postmortem computed tomography
*Statistically significant

Table 19. Inner and outer aortic wall area measurements on antemortem CT and postmortem CT

	Outer				Inner				
	AMCT	PMCT	p value	PM/AM	AMCT	PMCT	p value	PM/AM	p value#
(cm^2; mean±SD)	6.1±1.7	4.2±1.4	<0.0001*	0.70±0.14	4.3±1.3	2.5±0.9	<0.0001*	0.57±0.14	<0.0001*

Statistical analyses were performed by paired t-test.
SD, standard deviation; Outer, the area within the outer aortic wall; Inner, the area within the inner aortic wall; AMCT, antemortem computed tomography; PMCT, postmortem computed tomography; PM/AM, ratio of the cross-sectional area of the aortic wall on postmortem computed tomography to that on antemortem computed tomography
p value#, between PM/AM of outer aorta and that of inner aorta
*Statistically significant

Table 20. Cross-sectional area of the aortic wall on antemortem CT and postmortem CT

	AMCT	PMCT	p value
(cm^2; mean±SD)	1.8±0.8	1.8±0.7	0.89

Statistical analyses were performed by paired t-test.
SD, standard deviation; AMCT, antemortem computed tomography; PMCT, postmortem computed tomography

Discussion

While several previous studies have evaluated the postmortem changes of the cardiovascular system, few studies have focused on aortic wall thickness. Shiotani et al. [26] reported increased density of the aortic wall and smaller diameter of the ascending thoracic aorta on postmortem CT, compared with the CT findings in a different group of living persons. In their study, aortic wall thickness on postmortem CT was approximately 2 mm, which is in agreement with the present results; however, they made no comparison with aortic wall thickness on antemortem CT. The present study is the first to examine aortic wall thickness on CT before and after death in the same patients.

Takahashi et al. [28] reported that the aorta becomes oval in shape and its diameter is reduced on postmortem CT compared with corresponding antemortem images, which is reconfirmed by my study. Hyodoh et al. [25] provided quantitative evidence that the diameter of the aorta decreased by 81.3% along its long axis and by 68.0% in caliber on postmortem CT compared with antemortem CT images. They also showed that the postmortem cross-sectional area of the aorta was 60.8% of its antemortem size, which is consistent with the present results. It is reported that the arterial wall thickens and its components are compressed when the diameter of the artery decreases [52-54]. Assuming that the diameter of the aorta decreases after death, it is consistent that the aortic wall would become thicker post mortem, as was shown in the current study.

To compare the postmortem aortic thickening with other vessels, I further examined wall thickness of SVC on antemortem CT and postmortem CT. In contrast, wall thickness of SVC was significantly reduced post mortem. Since the diameter of SVC increases post mortem as Hyodoh et al. [25] and Shiotani et al. [27] showed, it is consistent that the wall of SVC would become thinner post mortem, as was shown in the current study.

I also investigated the correlation between postmortem change in aortic wall thickness and diameter of the aorta. Although no statistically significant correlation was found, it was qualitatively shown that vascular wall thickens as diameter of vessels decreases and vice versa, when taking both of the results in the aorta and SVC into consideration.

In the present study, the aortic wall was significantly thicker on postmortem CT than on antemortem CT in the same patients. This change may be related to “hyperattenuating aortic wall”, which was described by Shiotani et al. [26] as an aortic wall circumference that is continuously higher in attenuation than the lumen. They described that compression of aortic wall components such as collagen fiber, elastic fiber, and smooth muscle may contribute to hyperattenuation. The cross-sectional area of the aortic wall should be larger on postmortem CT than on antemortem CT if postmortem aortic wall thickening is caused by contraction of arterial smooth muscle as a part of rigor mortis. However, the results of the present study showed no change in cross-sectional area of the aortic wall between before and after death, which suggests that rigor mortis plays little role in postmortem aortic wall thickening.

It is possible that contrast substance in the body enhances the aortic wall after death and the partial volume effect produces a thicker wall of the aorta. However, contrast-enhanced antemortem CT was performed at 2-1395 days (median, 138 day) before death in this study, which was long enough for contrast medium to be eliminated from the body even in patients with severe renal impairment [55-57].

Because of the obvious differences in appearance between contrast-enhanced and plain images, I evaluated whether the measured values of aortic wall thickness were equivalent between these two sets of images. No significant difference was found, which enabled me to use either contrasted or non-contrasted images to obtain measurements.

My study has several limitations. First, breathing-induced motion of the carina during antemortem CT may have resulted in imprecise identification of the aortic wall for measurement. I assume, however, that the thickness of the continuous aortic wall is fundamentally constant regardless of a slight position shift. Second, motion artifact from the heart is a major concern on antemortem CT that clearly does not arise on postmortem CT. Third, I did not consider underlying disease, cause of death, preservation of cadavers, atmospheric temperature, or humidity, among other factors, which do affect postmortem changes [40, 41]. However, I consider that these factors would have had little effect on my conclusion because I excluded cardiovascular disease from analysis (which was also

confirmed by pathological autopsy) and all the cadavers were preserved under automatically regulated conditions at our hospital.

Conclusions

The area within the inner wall and the area within the outer wall reduce significantly after death, and the area within the inner wall changes more than within the outer wall. This is the first longitudinal study to elucidate that the aortic wall is significantly thicker on postmortem CT than on antemortem CT in cases of non-traumatic in-hospital death, and that the cross-sectional area of the aortic wall does not change between before and after death.

9. “Comparison of the cardiothoracic ratio between postmortem and antemortem computed tomography”

Background

The cardiothoracic ratio (CTR) is very simple to measure and is frequently used in clinical practice as a radiographic index of heart size. A CTR > 0.50 is generally defined as cardiomegaly. Some studies have assessed the CTR on antemortem CT [58, 59] or on postmortem CT [60, 61]. To my knowledge, however, no studies have compared the changes in CTR between antemortem and postmortem images in the same subjects. Because I often encounter radiological cardiomegaly on postmortem CT in patients with a pathologically normal heart, I hypothesized that the threshold CTR to detect cardiomegaly on postmortem CT may differ from the CTR on antemortem CT. Therefore, the objectives of this study were to describe the normal changes in CTR on postmortem CT in comparison with antemortem CT, and to compare the postmortem changes in CTR between different heart conditions. To achieve these objectives, I conducted a quantitative study in which I determined the changes in CTR between postmortem and antemortem CT scans obtained in the same subjects.

Materials and Methods

Study design and subjects

I retrospectively enrolled all consecutive subjects who died from nontraumatic causes in our academic tertiary care hospital and who underwent chest antemortem CT, postmortem CT, and autopsy between April 2009 and December 2011. A total of 167 consecutive subjects were initially included in this study. Subjects aged < 20 years and those with a history of congenital heart disease or cardiovascular surgery were excluded. After applying the exclusion criteria, 147 adults (100 males, 47 females) were included in this study. The mean age at death was 67 years (range, 21–92 years; median, 72 years). The subject disposition is shown in Fig. 8. Antemortem CT scanning was performed at a median of 14 days before death (range, 1–71 days). Postmortem CT scanning was performed at a median of 5.8 h after death (range, 1.2–23 h) and was immediately followed by autopsy.

All cadavers were carefully transported on a stretcher and were kept in the supine position at room temperature from the time of death until postmortem CT.

Image interpretation

All images were interpreted by a board-certified radiologist (8 years of experience) who was not provided with clinical information. The postmortem and most recent antemortem chest CT images were compared. CT images were reviewed on a two-dimensional workstation (OsiriX, Pixmeo Inc., Bernex, Switzerland). I measured the CTR on the scout view and axial

slices of each antemortem and postmortem CT by using the workstation caliper tool. The thoracic diameter was delineated by the inner borders of the thoracic cavity and the cardiac diameter was delineated by the outer borders of the heart. The two measurements were not necessarily made at the same level but were made parallel to each other (Fig. 9a-b).

Pathological analysis

In order to study the influence of morphological and functional changes in the heart on the postmortem changes in CTR caused by antemortem myocardial infarction and perimortem CPR, the subjects were divided into three groups based on the following pathological findings and clinical information: normal hearts, hearts with old myocardial infarction, and CPR-treated hearts. Normal heart was defined as the absence of gross pathological findings and space-occupying lesions. The pathological diagnosis of old myocardial infarction was confirmed microscopically if the macroscopic autopsy or postmortem CT findings were unclear. The cause of death was determined based on the subject's antemortem clinical course and the postmortem pathological findings. All hearts were weighed at autopsy and classified as normal or cardiomegaly according to the normative values reported by Zeek et al. [62], who weighed the hearts of a normal population and generated normal heart weight tables for males and females. Cardiomegaly was defined as a heart weight at least two standard deviations above the mean.

Statistical analyses

CTR measured on an axial image (CTRa) was compared with CTR measured on the scout view (CTRs) using paired *t* tests. The CTR on antemortem CT was compared with the CTR on postmortem CT using paired *t* tests. The postmortem change in CTR was calculated as the CTR on postmortem CT divided by the CTR on antemortem CT. The postmortem changes in CTR were compared among the three groups of subjects (i.e. normal hearts, hearts with old myocardial infarction, and CPR-treated hearts) using the Kruskal–Wallis test. I used unpaired *t* tests to compare the postmortem changes in CTR between sexes, and linear least squares regression was used to examine the effects of age and the time elapsed since death on CTR. The Kruskal–Wallis test was also used to determine the association between the cause of death and the postmortem changes in CTR in the three groups of subjects.

The diagnostic performance of CTR for detecting hearts with cardiomegaly (defined as heart weight of at least two standard deviations above the mean) was assessed and the sensitivity and specificity were calculated with 95% confidence intervals (CI). Receiver-operating characteristic (ROC) curves were plotted to evaluate the use of CTR for detecting cardiomegaly. Point estimates, 95% CIs, and the areas under the ROC curve (AUC) were calculated.

The level of statistical significance was set at 0.05. All statistical analyses were performed using R version 3.3.1 (The R Foundation for Statistical Computing).

Fig. 8. Subject disposition

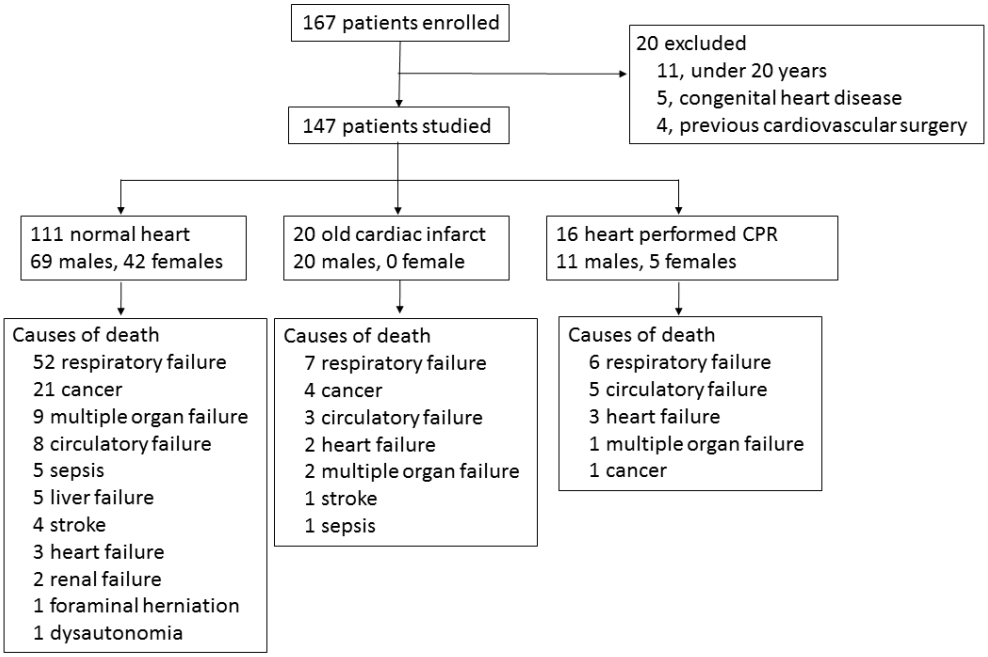

Fig. 9. Measurement of the cardiothoracic ratio (CTR) on scout (a) and axial (b) images.

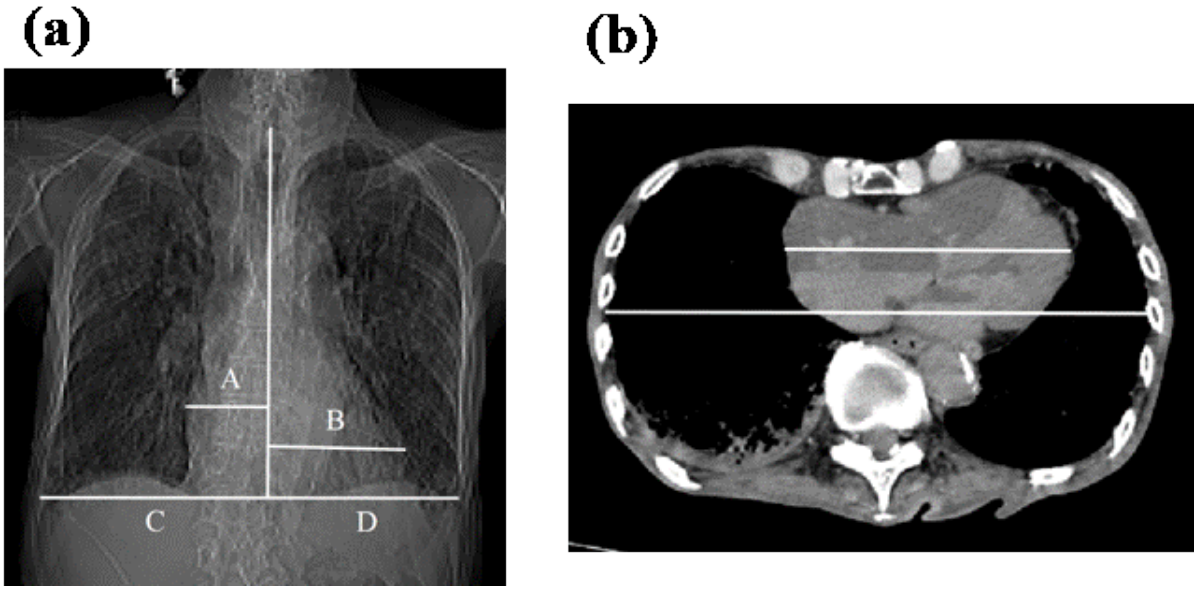

The thoracic diameter is delineated by the inner borders of the thoracic cavity and the heart diameter is delineated by the outer borders of the heart. The two measurements were not necessarily made at the same level but they were made parallel to each other. The CTR on scout images was calculated as follows: CTR = (A+B) / (C+D).

Results

The mean heart weight was 389.3 ± 117.7 g in all subjects, 420.2 ± 117.7 g in males, and 336.5 ± 90.7 g in females, and ranged from 193 to 926 g. For each case, the normative value range was estimated based using the formula reported by Zeek et al. [62]: 1.9 times the body length in centimeters minus 2.1 plus or minus 40 for males, and 1.78 times the body length in centimeters minus 21.58 plus or minus 30 for females. Based on this formula, 78/147 hearts were enlarged in my study.

The CTRs and CTRa determined on antemortem and postmortem CT in each group are reported in Table 21 and are shown graphically in Figure 10. CTRs was significantly greater than CTRa on antemortem CT in the normal heart ($P < 0.001$) and old myocardial infarction ($P = 0.02$) groups, and on postmortem CT in the normal heart ($P < 0.001$) and CPR-treated heart ($P < 0.01$) groups. CTRs tended to be greater than CTRa on antemortem CT in the CPR-treated heart group and on postmortem CT in the old myocardial infarction group, although these differences were not statistically significant.

The ratios of CTRs and CTRa on postmortem CT to those on antemortem CT in each group are shown in Table 22. The mean ratio of CTRs on postmortem CT to CTRs on antemortem CT was 1.08 (range, 1.07 to 1.10); CTRs on postmortem CT was significantly greater than CTRs on antemortem CT in all three groups ($P < 0.01$). The ratio of CTRs between antemortem and postmortem CT was not significantly different among the three groups of

subjects (P = 0.85). The mean ratio of CTRa on postmortem CT to CTRa on antemortem CT was 1.07 (range, 1.06 to 1.08); CTRa on postmortem CT was significantly greater than CTRa on antemortem CT in all three groups (P < 0.01). The ratio of CTRa between antemortem and postmortem CT was not significantly different among the three groups of subjects (P = 0.81).

Sex was not significantly associated with the postmortem change in CTR in any group (Table 23). Because the old myocardial infarction group only included males, statistical analyses were not possible. Table 24 shows the results of correlation analyses of the postmortem change in CTR with age, time elapsed since death, and the cause of death. The postmortem change in CTR was not significantly correlated with any of these variables in any group.

Figure 11 shows the result of the ROC curve analysis. The area under the ROC curve was 0.71 (95% CI 0.63–0.79). A CTR threshold of 0.50 had a sensitivity of 86% and specificity of 32% for the detection of cardiomegaly. Increasing the CTR threshold to 0.54 increased the specificity to 75% and the sensitivity to 63%.

Table 21. Antemortem and postmortem cardiothoracic ratios measured on scout and axial CT images

		Normal hearts	Hearts with old myocardial infarction	CPR-treated hearts
Antemortem	CTRs	0.52 ± 0.07	0.53 ± 0.07	0.52 ± 0.08
	CTRa	0.50 ± 0.06	0.51 ± 0.07	0.50 ± 0.06
	P value*	< 0.001	0.02	0.07
	CTRs/CTRa	1.043	1.027	1.045
Postmortem	CTRs	0.55 ± 0.08	0.57 ± 0.08	0.57 ± 0.07
	CTRa	0.53 ± 0.06	0.56 ± 0.06	0.53 ± 0.07
	P value*	< 0.001	0.12	< 0.01
	CTRs/CTRa	1.056	1.025	1.076

Values are presented as the mean ± standard deviation.
*Paired *t* test for CTRs versus CTRa.
CT, computed tomography; CTRs, cardiothoracic ratio on the scout view; CTRa, cardiothoracic ratio on an axial image; CTRs/CTRa, ratio of CTRs to CTRa

Table 22. Comparison of cardiothoracic ratios between postmortem and antemortem CT

		Normal hearts	Hearts with old myocardial infarction	CPR-treated hearts
CTRs	PM/AM	1.07 ± 0.16	1.07 ± 0.11	1.10 ± 0.14
	P value*	< 0.001	< 0.01	0.01
CTRa	PM/AM	1.06 ± 0.11	1.08 ± 0.10	1.07 ± 0.09
	P value†	< 0.001	< 0.01	< 0.01

Values are presented as the mean ± standard deviation.
*Paired *t* test for antemortem CTRs versus postmortem CTRs.
†Paired *t* test for antemortem CTRa versus postmortem CTRa.
CT, computed tomography; CTRs, cardiothoracic ratio on the scout view; CTRa, cardiothoracic ratio on an axial image; PM/AM, ratio of CTR on postmortem CT to CTR on antemortem CT.

Fig. 10. Bar graphs of antemortem and postmortem cardiothoracic ratios on scout (a) and axial (b) images.

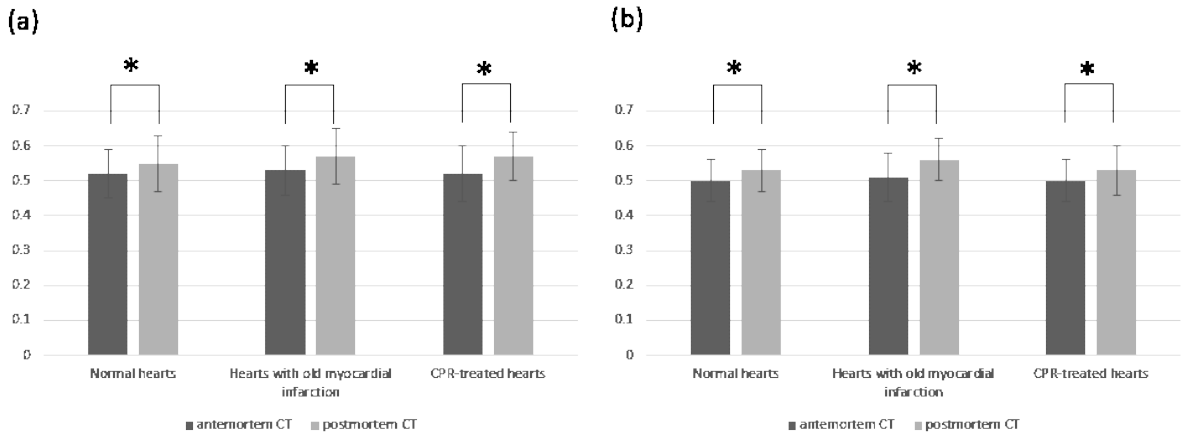

*Statistically significant

Table 23. Association between cardiothoracic ratio and sex

	Normal hearts	Hearts with old myocardial infarction	CPR-treated hearts
Male	1.07 ± 0.11	1.08 ± 0.10	1.05 ± 0.09
Female	1.06 ± 0.09	N/A	1.08 ± 0.09
P value*	0.61	N/A	0.55

Values are presented as the mean ± standard deviation.
*Unpaired *t* test.

Table 24. Correlations of cardiothoracic ratio with age, time elapsed since death, and cause of death.

	Normal hearts	Hearts with old myocardial infarction	CPR-treated hearts
Age	0.18	0.99	0.30
Time elapsed since death	0.20	0.57	0.22
Cause of death	0.69	0.29	0.24

Values are presented as the *P* value, and were determined by linear least squares regression (age and time elapsed since death) or the Kruskal–Wallis test (cause of death).

Fig. 11. Receiver-operating characteristic curve of using the postmortem cardiothoracic ratio for the detection of cardiomegaly.

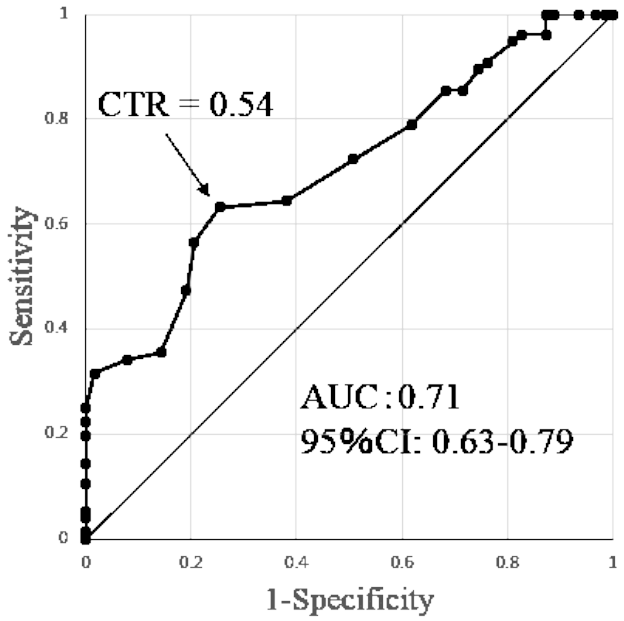

The area under the ROC curve was 0.71 (95% CI 0.63–0.79).
AUC, area under the curve; CI, confidence interval.

Discussion

A threshold CTR of 0.5 is commonly used as the cutoff value for cardiomegaly on plain chest radiography (CXR) in the standing position. Some studies have assessed and adapted the CTR approach in CT, and found that CTR on CXR in the standing position is strongly correlated with the CTR on CT, and that a threshold CTR of 0.5 could be used to detect cardiomegaly on CT [58, 59]. Winklhofer et al. chose the ratio of 0.57 as the cutoff value for cardiomegaly on postmortem CT [61]. The CTR measured on antemortem and postmortem CT in this study was therefore consistent with the values used in these earlier studies.

The CTR measured on the scout view was significantly overestimated relative to the CTR measured on an axial image. One reason for this is that pleural and pericardial effusion and masses neighboring the heart make it difficult to delineate the heart on CXR and on the scout view. In this study, 10 cases showed unclear delineation due to pleural and pericardial effusion and masses neighboring the heart, where I actually tended to overestimate the CTR. Another reason is that the scout view images have too low contrast and spatial resolutions hindering efforts to measure the exact diameter of the heart. For these reasons, I emphasize the importance of measurements on an axial image rather than those on the scout view. However, the scout view has important roles. In particular, it can be used to quickly determine which image level depicts the maximum diameter of the heart. Here, I used the CTR

determined on an axial image in my analyses because it is more accurate than the CTR determined on the scout view.

CTR measured on postmortem CT was significantly greater than the CTR on antemortem CT. Antemortem chest CT is usually performed in the inspiratory phase while postmortem CT is thought to be similar to CT in the expiratory phase [63]. In a study by Tomita et al., the mean CTR values determined in the expiratory and inspiratory phases were 0.49 ± 0.05 and 0.44 ± 0.05, respectively [64]. Therefore, the CTR on expiratory CT was 1.1 times greater than that on inspiratory CT. Considering these findings, the postmortem increase in CTR could be partly explained by the difference in respiratory phase between antemortem and postmortem CT. If this is the case, it is very important for us to recognize that the CTR on postmortem CT is generally greater than the CTR on antemortem chest CT, which is always measured in the inspiratory phase. Accordingly, we must be cautious when applying different thresholds to detect cardiomegaly on antemortem and postmortem CT. However, it has been shown that the heart wall becomes thicker postmortem [15] and the heart dilates, especially on the right side, postmortem [27]. These postmortem changes might also account for the enlarged CTR on postmortem CT.

CTR on postmortem images may be affected by morphological and functional changes in the heart caused by antemortem myocardial infarction and perimortem CPR. This is because necrosis or fibrosis of cardiac muscle due to old myocardial infarction can influence normal

postmortem changes such as heart wall thickening and heart dilation, which may result in a smaller CTR. By comparison, CPR causes hearts to be compressed and crushed, which may result in a larger CTR. However, I found no significant differences in the postmortem changes in CTR between the normal heart, old myocardial infarction, and CPR-treated heart groups. These results suggest that the postmortem changes in the heart are not just due to diseases or treatment in antemortem and perimortem periods.

I also investigated possible confounding factors for postmortem changes such as sex, age, and the cause of death. However, I found no statistically significant associations between these confounding factors and the postmortem changes in CTR. Overall, these results indicate that an increased CTR is a general postmortem finding that is independent of the subject's sex, age, cause of death, the presence of old myocardial infarction, and perimortem CPR.

The ROC curve analysis showed that CTR on postmortem CT could predict cardiomegaly with moderate accuracy. At a threshold of 0.50, which is widely used in CXR, the sensitivity was acceptable but the specificity was very low. When I increased the CTR threshold to 0.54, the specificity increased and the ability to diagnose cardiomegaly was improved. Considering that the CTR threshold of 0.50 on antemortem CT can detect cardiomegaly [58, 59], and that postmortem thickening of the heart wall [15] and dilation of the heart [27] are associated with increases in CTR on postmortem images, as shown in my study, the CTR threshold of 0.54 for detecting cardiomegaly on postmortem CT seems to be reasonable.

The main limitation of this study is that underlying diseases or cadaver storage might contribute to the postmortem changes observed [40, 41]. However, these factors are unlikely to affect my conclusions because I divided the subjects into three groups based on their pathological and clinical information; namely subjects with a normal heart, subjects with old myocardial infarction, and subjects who received CPR. Furthermore, all of the cadavers were preserved at our hospital in the same place, at the same temperature, and in the same position.

Conclusions

My study revealed that the CTR was significantly greater on postmortem CT images than on antemortem CT images in three groups of subjects, namely subjects with a normal heart, subjects with old myocardial infarction, and subjects who underwent CPR. My results also suggest that measuring the CTR on axial postmortem CT images can aid the diagnosis of cardiomegaly. However, it is important to avoid overestimating cardiomegaly because CTR generally increases postmortem, and we need to establish new criteria for interpreting postmortem CTR in this context.

10. Overall discussion

(a) Interscanner variability

Because I used different CT scanners for antemortem and postmortem CT, I scanned the same imaging phantom to verify the feasibility of comparing attenuation among machines before comparing CT attenuation between antemortem and postmortem CT. I scanned the chest portion of a whole-body imaging phantom (PBU-60, Kyoto Kagaku Co., Ltd., Kyoto, Japan) and measured attenuation of the same area of the heart with a 20 cm^2 circular region of interest. These values are shown in Table 25. The results suggest that the differences in CT attenuation between individual machines are small enough to enable comparison of the antemortem and postmortem CT attenuation values obtained using different scanners.

Regarding other parameters, higher exposure dose is known to decrease image noise [65]. While one study revealed that CT attenuation is independent of tube current [49], another experimental study showed that CT attenuation is dependent on tube voltage and the authors reported that the differences in CT attenuation between scanners were smaller at 120 kV than at 80 kV [66]. In the present research, the tube voltage was set to 120 kV for all scanners but the tube current was variable. This may support the results of the imaging phantom analysis, which revealed very small differences in CT attenuation between the individual scanners.

(b) Appropriateness of the measurements

One concern of unenhanced CT is whether it provides adequate measurement of the heart and aortic wall thicknesses, as contrast is commonly insufficient to enable distinction between the target structure and other neighboring structures, and it can be difficult to judge where to measure the structure on unenhanced CT. However, the profile curve for the aortic wall (Fig. 12) indicates that there were clear differences in intensity between the target structure and the neighboring structures, providing assurance regarding the appropriateness of the measurements taken in this study.

Another concern may be inter-rater reliability when multiple raters take measurements. In chapters 6 and 8, the images were analyzed by two board-certified radiologists and the best fit was determined by agreement between the radiologists. If more raters are involved in larger-scale studies, any inter-rater differences could significantly affect the results. Computer-assisted and automated measurements may help to overcome this issue.

(c) Correlation between CT attenuation and thickness of the heart wall

In a preliminary analysis, I investigated whether the postmortem change in CT attenuation was correlated with the thickness of the heart wall by paired t-test. However, these variables were not significantly correlated (P=0.90). One reason may be that the individual differences between antemortem and postmortem imaging are greater than the change observed for the overall group. Another reason may be that the number of patients included in the study was

too small to detect significant differences. More reliable results could be obtained if greater numbers of patients are included in future studies.

Table 25. Comparison of CT attenuation in an imaging phantom among three scanners

Scanner	Aquillion 64	Discovery CT 750 HD	Robusto
CT attenuation (HU)	34.49	34.64	34.77

CT, computed tomography; HU, Hounsfield units

Fig. 12 Profile curve of the aortic wall

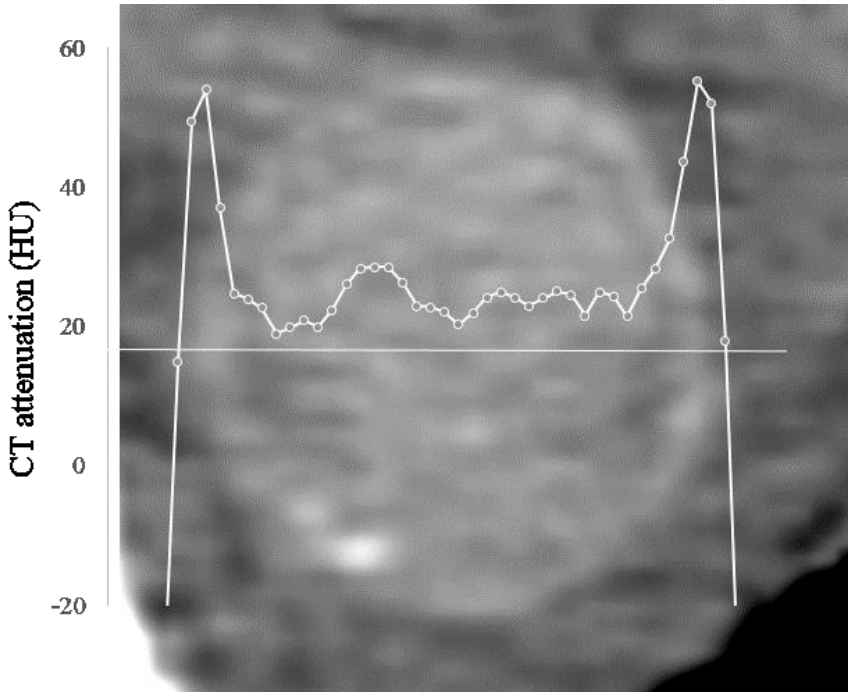

11. Conclusions

I have conducted four consecutive studies examining the postmortem changes of the following cardiovascular features: thickness of the heart wall, attenuation of cardiac muscle, the cardiothoracic ratio, and the thickness of the aortic wall. I found that the thickness of the heart wall, attenuation of cardiac muscle, cardiothoracic ratio, and thickness of the aortic wall were generally greater on postmortem CT than on antemortem CT in the same patients. These results caution us against overestimating cardiomegaly and incorrectly labeling normal postmortem changes of the cardiovascular system as being pathological.

Postmortem CT is increasingly being used to investigate the cause of death. Postmortem CT is now used to determine the cause of death in about 30% of cases. Although the postmortem CT findings were not significantly associated with the causes of death in this study, ongoing efforts to clarify the relationship between postmortem CT findings and the underlying causes should improve the accuracy of using postmortem CT to determine the cause of death. It is very important to accumulate further knowledge about the normal postmortem imaging features, and some of these postmortem changes were described in this research. I believe that the results reported here will help us to establish guidelines for the interpretation of postmortem CT images.

The time elapsed since death is currently assessed based on external features of the body. Although I tried to estimate the time elapsed since death using postmortem CT data, I found

no significant correlations between the postmortem changes in any of the assessed features and the time elapsed since death. If some postmortem changes are correlated with the time elapsed since death, it may be possible to estimate the time of death in terms of the image features. If this proves possible, I believe it will provide a major milestone in the field of forensic medicine.

The field of postmortem imaging is still developing and most radiologists, clinical pathologists, and forensic pathologists have limited experience in interpreting postmortem images. It is important that these experts can recognize specific features on postmortem images. Further studies on postmortem imaging, especially of the normal postmortem changes, are needed.

12. Acknowledgements

I thank the executives of our hospital for supporting the maintenance of the CT scanners, the clinical doctors in the relevant hospital departments for obtaining informed consent from each subject's next of kin and for mediating between the subjects and my study group.

This work was supported by a grant from the Japanese Ministry of Health, Labor and Welfare for research into "Usefulness of Postmortem Images as an Ancillary Method for Autopsy in Evaluation of Death Associated with Medical Practice (2008–2009)".

13. References

1. Shojania KG, Burton EC, McDonald KM, Goldman L. Changes in rates of autopsy-detected diagnostic errors over time: a systematic review. Jama. 289:2849-56. 2003.

2. Thali MJ, Yen K, Schweitzer W, Vock P, Boesch C, Ozdoba C, et al. Virtopsy, a new imaging horizon in forensic pathology: virtual autopsy by postmortem multislice computed tomography (MSCT) and magnetic resonance imaging (MRI)--a feasibility study. J Forensic Sci. 48:386-403. 2003.

3. O'Donnell C, Woodford N. Post-mortem radiology--a new sub-speciality? Clin Radiol. 63:1189-94. 2008.

4. Cha JG, Kim DH, Kim DH, Paik SH, Park JS, Park SJ, et al. Utility of postmortem autopsy via whole-body imaging: initial observations comparing MDCT and 3.0 T MRI findings with autopsy findings. Korean J Radiol. 11:395-406. 2010.

5. Roberts IS, Benamore RE, Benbow EW, Lee SH, Harris JN, Jackson A, et al. Post-mortem imaging as an alternative to autopsy in the diagnosis of adult deaths: a validation study. Lancet. 379:136-42. 2012.

6. Flach PM, Thali MJ, Germerott T. Times have changed! Forensic radiology--a new challenge for radiology and forensic pathology. AJR Am J Roentgenol. 202:W325-34. 2014.

7. Shiotani S, Kohno M, Ohashi N, Atake S, Yamazaki K, Nakayama H. Cardiovascular gas on non-traumatic postmortem computed tomography (PMCT): the influence of cardiopulmonary resuscitation. Radiat Med. 23:225-9. 2005.

8. Shiotani S, Kohno M, Ohashi N, Yamazaki K, Itai Y. Postmortem intravascular high-density fluid level (hypostasis): CT findings. J Comput Assist Tomogr. 26:892-3. 2002.

9. Shiotani S, Kohno M, Ohashi N, Yamazaki K, Nakayama H, Watanabe K. Postmortem computed tomographic (PMCT) demonstration of the relation between gastrointestinal (GI) distension and hepatic portal venous gas (HPVG). Radiat Med. 22:25-9. 2004.

10. Shiotani S, Kohno M, Ohashi N, Yamazaki K, Nakayama H, Watanabe K, et al. Non-traumatic postmortem computed tomographic (PMCT) findings of the lung. Forensic science international. 139:39-48. 2004.

11. Christe A, Flach P, Ross S, Spendlove D, Bolliger S, Vock P, et al. Clinical radiology and postmortem imaging (Virtopsy) are not the same: Specific and unspecific postmortem signs. Leg Med (Tokyo). 12:215-22. 2010.

12. Ishida M, Gonoi W, Okuma H, Shirota G, Shintani Y, Abe H, et al. Common Postmortem Computed Tomography Findings Following Atraumatic Death: Differentiation between Normal Postmortem Changes and Pathologic Lesions. Korean J Radiol. 16:798-809. 2015.

13. Ishida M, Gonoi W, Hagiwara K, Takazawa Y, Akahane M, Fukayama M, et al. Hypostasis in the heart and great vessels of non-traumatic in-hospital death cases on

postmortem computed tomography: relationship to antemortem blood tests. Leg Med (Tokyo). 13:280-5. 2011.

14. Ishida M, Gonoi W, Hagiwara K, Takazawa Y, Akahane M, Fukayama M, et al. Intravascular gas distribution in the upper abdomen of non-traumatic in-hospital death cases on postmortem computed tomography. Leg Med (Tokyo). 13:174-9. 2011.

15. Okuma H, Gonoi W, Ishida M, Shintani Y, Takazawa Y, Fukayama M, et al. Heart wall is thicker on postmortem computed tomography than on antemortem [corrected] computed tomography: the first longitudinal study. PLoS One. 8:e76026. 2013.

16. Okuma H, Gonoi W, Ishida M, Shintani Y, Takazawa Y, Fukayama M, et al. Greater thickness of the aortic wall on postmortem computed tomography compared with antemortem computed tomography: the first longitudinal study. Int J Legal Med. 128:987-93. 2014.

17. Shirota G, Gonoi W, Ishida M, Okuma H, Shintani Y, Abe H, et al. Brain Swelling and Loss of Gray and White Matter Differentiation in Human Postmortem Cases by Computed Tomography. PLoS One. 10:e0143848. 2015.

18. Ishida M, Gonoi W, Hagiwara K, Takazawa Y, Akahane M, Fukayama M, et al. Postmortem changes of the thyroid on computed tomography. Leg Med (Tokyo). 13:318-22. 2011.

19. Ishida M, Gonoi W, Hagiwara K, Okuma H, Shirota G, Shintani Y, et al. Early postmortem volume reduction of adrenal gland: initial longitudinal computed tomographic study. Radiol Med. 120:662-9. 2015.

20. Okuma H, Gonoi W, Ishida M, Shirota G, Kanno S, Shintani Y, et al. Comparison of volume and attenuation of the spleen between postmortem and antemortem computed tomography. Int J Legal Med. 130:1081-7. 2016.

21. Okuma H, Gonoi W, Ishida M, Shirota G, Shintani Y, Abe H, et al. Comparison of attenuation of striated muscle between postmortem and antemortem computed tomography: results of a longitudinal study. PLoS One. 9:e111457. 2014.

22. Ishida M, Gonoi W, Hagiwara K, Okuma H, Shintani Y, Abe H, et al. Fluid in the airway of nontraumatic death on postmortem computed tomography: relationship with pleural effusion and postmortem elapsed time. Am J Forensic Med Pathol. 35:113-7. 2014.

23. Arthurs OJ, Guy A, Kiho L, Sebire NJ. Ventilated postmortem computed tomography in children: feasibility and initial experience. Int J Legal Med. 129:1113-20. 2015.

24. Yutani C, editor. Atlas of cardiovascular epathology. Bunkyodo, Tokyo. 3-16. 2002.

25. Hyodoh H, Sato T, Onodera M, Washio H, Hasegawa T, Hatakenaka M. Vascular measurement changes observed using postmortem computed tomography. Japanese journal of radiology. 30:840-5. 2012.

26. Shiotani S, Kohno M, Ohashi N, Yamazaki K, Nakayama H, Ito Y, et al. Hyperattenuating aortic wall on postmortem computed tomography (PMCT). Radiat Med. 20:201-6. 2002.

27. Shiotani S, Kohno M, Ohashi N, Yamazaki K, Nakayama H, Watanabe K, et al. Dilatation of the heart on postmortem computed tomography (PMCT): comparison with live CT. Radiat Med. 21:29-35. 2003.

28. Takahashi N, Higuchi T, Hirose Y, Yamanouchi H, Takatsuka H, Funayama K. Changes in aortic shape and diameters after death: comparison of early postmortem computed tomography with antemortem computed tomography. Forensic science international. 225:27-31. 2013.

29. Hutchins GM, Bulkley BH, Moore GW, Piasio MA, Lohr FT. Shape of the human cardiac ventricles. The American journal of cardiology. 41:646-54. 1978.

30. Levy AD, Harcke HT, Mallak CT. Postmortem imaging: MDCT features of postmortem change and decomposition. Am J Forensic Med Pathol. 31:12-7. 2010.

31. Joseph DR, Meltzer S. The postmortem rigor of the mammalian heart and the influence of an antemortem stimulation of the pneumogastric nerves upon its development. The Journal of experimental medicine. 11:10-35. 1909.

32. MacWilliam JA. Rigor mortis in the heart and the state of the cardiac cavities after death. The Journal of physiology. 27:336. 1901.

33. Smith RD. Studies on rigor mortis. Part II. Qualitative observations on the post mortem shortening of muscles. The Anatomical record. 108:207-16. 1950.

34. Tsokos M. Postmortem changes. Encyclopedia of forensic and legal medicine. 3:456-76. 2005.

35. Maron BJ, Towbin JA, Thiene G, Antzelevitch C, Corrado D, Arnett D, et al. Contemporary definitions and classification of the cardiomyopathies an American heart association scientific statement from the council on clinical cardiology, heart failure and transplantation committee; quality of care and outcomes research and functional genomics and translational biology interdisciplinary working groups; and council on epidemiology and prevention. Circulation. 113:1807-16. 2006.

36. Schoen FJ, Mitchell RN. Cardiomyopathies. In: Kumar V, Abbas AK, Fausto N, Aster JC, editors. Pathologic Basis of Disease. Saunders. 571-581. 2010.

37. Somsen GA, Hovingh GK, Tulevski I, Seidman J, Seidman CE. Familial dilated cardiomyopathy. Clinical Cardiogenetics: Springer. 63-77. 2011.

38. Hall J. Cardiac muscle; the heart as a pump and function of the heart valves. JE Hall Textbook of Medical Physiology Philadelphia: Saunders.101-13. 2011.

39. Sato T, Yamanari H, Ohe T, Yoshinouchi T. Regional left ventricular contractile dynamics in hypertrophic cardiomyopathy evaluated by magnetic resonance imaging. Heart and vessels. 11:248-54. 1996.

40. Jackowski C, Sonnenschein M, Thali MJ, Aghayev E, Yen K, Dirnhofer R, et al. Intrahepatic gas at postmortem computed tomography: forensic experience as a potential guide for in vivo trauma imaging. J Trauma. 62:979-88. 2007.

41. Singh MK, O'Donnell C, Woodford NW. Progressive gas formation in a deceased person during mortuary storage demonstrated on computed tomography. Forensic Sci Med Pathol. 5:236-42. 2009.

42. Mull RT. Mass estimates by computed tomography: physical density from CT numbers. AJR Am J Roentgenol. 143:1101-4. 1984.

43. Hadar H, Gadoth N, Heifetz M. Fatty replacement of lower paraspinal muscles: normal and neuromuscular disorders. AJR Am J Roentgenol. 141:895-8. 1983.

44. Hawley RJ, Jr., Schellinger D, O'Doherty DS. Computed tomographic patterns of muscles in neuromuscular diseases. Archives of neurology. 41:383-7. 1984.

45. Bulcke JA, Termote JL, Palmers Y, Crolla D. Computed tomography of the human skeletal muscular system. Neuroradiology. 17:127-36. 1979.

46. Termote JL, Baert A, Crolla D, Palmers Y, Bulcke JA. Computed tomography of the normal and pathologic muscular system. Radiology. 137:439-44. 1980.

47. Groell R, Rienmueller R, Schaffler GJ, Portugaller HR, Graif E, Willfurth P. CT number variations due to different image acquisition and reconstruction parameters: a thorax phantom study. Comput Med Imaging Graph. 24:53-8. 2000.

48. Levi C, Gray JE, McCullough EC, Hattery RR. The unreliability of CT numbers as absolute values. AJR Am J Roentgenol. 139:443-7. 1982.

49. Birnbaum BA, Hindman N, Lee J, Babb JS. Multi-detector row CT attenuation measurements: assessment of intra- and interscanner variability with an anthropomorphic body CT phantom. Radiology. 242:109-19. 2007.

50. Nishihara S, Koike M, Ueda K, Sanada T, Ebitani K. Intra- and inter-equipment variations in the mean CT numbers of a vertebral body for X-ray CT equipment. Med Imag Inform Sci. 20:40-3. 2002.

51. Yamazaki K, Shiotani S, Ohashi N, Doi M, Honda K. Hepatic portal venous gas and hyper-dense aortic wall as postmortem computed tomography finding. Leg Med (Tokyo). 5 Suppl 1:S338-41. 2003.

52. Burton A. Arrangements of many vessels. Physiology and Biophysics of the Circulation Year Book Medical Publishers, Chicago.51-62. 1973.

53. Burton A. Walls of the blood vessels and their function. Physiology and Biophysics of the Circulation Year Book Medical Publishers, Chicago.63-75. 1973.

54. Folkow B, editor. Vascular length and radius. In: Folkow B, Neil E, editors. Circulation. Oxford University Press, New York. 45-56. 1971.

55. Corradi A, Menta R, Cambi V, Maccarini P, Cerutti R. Pharmacokinetics of iopamidol in adults with renal failure. Arzneimittel-Forschung. 40:830-2. 1990.

56. Lehnert T, Keller E, Gondolf K, Schaffner T, Pavenstadt H, Schollmeyer P. Effect of haemodialysis after contrast medium administration in patients with renal insufficiency. Nephrology, dialysis, transplantation : official publication of the European Dialysis and Transplant Association - European Renal Association. 13:358-62. 1998.

57. Lorusso V, Taroni P, Alvino S, Spinazzi A. Pharmacokinetics and safety of iomeprol in healthy volunteers and in patients with renal impairment or end-stage renal disease requiring hemodialysis. Investigative radiology. 36:309-16. 2001.

58. Miller J, Singer A, Hinrichs C, Contractor S, Doddakashi S. Cardiac dimensions derived from helical CT: correlation with plain film radiography. Internet J Radiol. 1. 2000.

59. Gollub MJ, Panu N, Delaney H, Sohn M, Zheng J, Moskowitz CS, et al. Shall we report cardiomegaly at routine computed tomography of the chest? J Comput Assist Tomogr. 36:67-71. 2012.

60. Jotterand M, Doenz F, Grabherr S, Faouzi M, Boone S, Mangin P, et al. The cardiothoracic ratio on post-mortem computer tomography. Int J Legal Med. 130:1309-13. 2016.

61. Winklhofer S, Berger N, Ruder T, Elliott M, Stolzmann P, Thali M, et al. Cardiothoracic ratio in postmortem computed tomography: reliability and threshold for the diagnosis of cardiomegaly. Forensic Sci Med Pathol. 10:44-9. 2014.

62. Zeek PM. Heart weight. I. The weight of the normal human heart. Arch Pathol. 34:820-32. 1942.

63. Robinson C, Biggs MJ, Amoroso J, Pakkal M, Morgan B, Rutty GN. Post-mortem computed tomography ventilation; simulating breath holding. Int J Legal Med. 128:139-46. 2014.

64. Tomita H, Yamashiro T, Matsuoka S, Matsushita S, Kurihara Y, Nakajima Y. Changes in Cross-Sectional Area and Transverse Diameter of the Heart on Inspiratory and Expiratory Chest CT: Correlation with Changes in Lung Size and Influence on Cardiothoracic Ratio Measurement. PLoS One. 10:e0131902. 2015.

65. Lechuga L, Weidlich GA. Cone Beam CT vs. Fan Beam CT: A Comparison of Image Quality and Dose Delivered Between Two Differing CT Imaging Modalities. Cureus. 8:e778. 2016.

66. Sande EP, Martinsen AC, Hole EO, Olerud HM. Interphantom and interscanner variations for Hounsfield units--establishment of reference values for HU in a commercial QA phantom. Physics in medicine and biology. 55:5123-35. 2010.